(Nakayama *et al.*, 2004). For every section, a negative control with normal rabbit IgG was processed simultaneously. Sections were counterstained with hematoxylin and eosin.

Acknowledgments

We thank Midori Ikezaki and Akiko Emura for technical assistance. This work was supported in part by Grants-in-Aid from the Japanese Ministry of Education, Culture, Sports, Science, and Technology.

Abbreviations

BSA, bovine serum albumin; CMW, C-mannosylated tryptophan; ELISA, enzyme-linked immunosorbent assay; FITC, fluorescein isothiocyanate; KLH, keyhole limpet heamocyanine; MALDI, matrix-assisted laser desorption ionization; PBS, phosphate buffered saline; SDS–PAGE, sodium dodecyl sulfate–polyacrylamide gel electrophoresis; TSP, thrombospondin.

References

Adams, J.C. (2001) Thrombospondins: multifunctional regulators of cell interactions. *Annu. Rev. Cell. Dev. Biol.*, **17**, 25–51.

Akimoto, Y., Kreppel, L.K., Hirano, H., and Hart, G.W. (2000) Increased O-GlcNAc transferase in pancreas of rats with streptozotocin-induced diabetes. *Diabetologia*, **43**, 1239–1247.

Akimoto, Y., Kreppel, L.K., Hirano, H., and Hart, G.W. (2001) Hyperglycemia and the O-GlcNAc transferase in rat aortic smooth muscle cells: elevated expression and altered patterns of O-GlcNAcylation. *Arch. Biochem. Biophys.*, **389**, 166–175.

Bar-On, H., Nesher, G., Teitelbaum, A., and Ziv, E. (1997) Dolichol-mediated enhanced protein N-glycosylation in experimental diabetes—a possible additional deleterious effect of hyperglycemia. *J. Diabetes Complications*, **11**, 236–242.

Berry, E.M., Ziv, E., and Bar-On, H. (1980) Protein and glycoprotein synthesis and secretion by the diabetic liver. *Diabetologia*, **19**, 535–540.

Chibber, R., Ben-Mahmud, B.M., Mann, G.E., Zhang, J.J., and Kohner, E.M. (2003) Protein kinase C β2-dependent phosphorylation of core 2 GlcNAc-T promotes leukocyte-endothelial cell adhesion. A mechanism underlying capillary occlusion in diabetic retinopathy. *Diabetes*, **52**, 1519–1527.

Clark, R.J., McDonough, P.M., Swanson, E., Trost, S.U., Suzuki, M., Fukuda, M., and Dillmann, W.H. (2003) Diabetes and the accompanying hyperglycemia impairs cardiomyocyte calcium cycling through increased nuclear O-GlcNAcylation. *J. Biol. Chem.*, **278**, 44230–44237.

Coimbra, T.M., Janssen, U., Grone, H.J., Ostendorf, T., Kunter, U., Schmidt, H., Brabant, G., and Floege, J. (2000) Early events leading to renal injury in obese Zucker (fatty) rats with type II diabetes. *Kidney Int.*, **57**, 167–182.

De Peredo, A.G., Klein, D., Macek, B., Hess, D., Peter-Katalinic, J., and Hofsteenge, J. (2002) C-mannosylation and O-fucosylation of thrombospondin type 1 repeats. *Mol. Cell. Proteomics*, **1**, 11–18.

Dennis, J.W., Granovsky, M., and Warren, C.E. (1999) Protein glycosylation in development and disease. *BioEssays*, **21**, 412–421.

Doucey, M.-A., Hess, D., Cacan, R., and Hofsteenge, J. (1998) Protein c-mannosylation is enzyme-catalysed and uses dolichyl-phosphate-mannose as a precursor. *Mol. Biol. Cell*, **9**, 291–300.

Elzie, C.A. and Murphy-Ullrich, J.E. (2004) The N-terminus of thrombospondin: the domain stands apart. *Int. J. Biochem. Cell Biol.*, **36**, 1090–1101.

Furmanek, A. and Hofsteenge, J. (2000) Protein c-mannosylation: facts and questions. *Acta Biochim. Polonica.*, **47**, 781–789.

Furmanek, A., Hess, D., Rogniaux, H., and Hofsteenge, J. (2003) The WSAWS motif is c-hexosylated in a soluble form of the erythropoietin receptor. *Biochemistry*, **42**, 8452–8458.

Furukawa, K., Roberts, D.D., Endo, T., and Kobata, A. (1989) Structural study of the sugar chains of human platelet thrombospondin. *Arch. Biochem. Biophys.*, **270**, 302–312.

Garcia, A., Lenis, L.A., Jimenez, C., Debitus, C., Quinoa, E., and Riguera, R. (2000) The occurrence of the human glycoconjugate C(2)-α-D-mannosylpyranosyl-L-tryptophan in marine ascidians. *Org. Lett.*, **2**, 2765–2767.

Gutsche, B., Grun, C., Scheutzow, D., and Herderich, M. (1999) Tryptophan glycoconjugates in food and human urine. *Biochem. J.*, **343**, 11–19.

Haltiwanger, R.S. and Lowe, J.B. (2004) Role of glycosylation in development. *Annu. Rev. Biochem.*, **73**, 491–537.

Hanover, J.A. (2001) Glycan-dependent signaling: O-linked N-acetylglucosamine. *FASEB J.*, **15**, 1865–1876.

Hanover, J.A., Lai, Z., Lee, G., Lubas, W.A., and Sato, S.M. (1999) Elevated O-linked N-acetylglucosamine metabolism in pancreatic β-cells. *Arch. Biochem. Biophys.*, **362**, 38–45.

Hartmann, S. and Hofsteenge, J. (2000) Properdin, the positive regulator of complement, is highly c-mannosylated. *J. Biol. Chem.*, **275**, 28569–28574.

Hofsteenge, J., Muller, D.R., de Beer, T., Loffler, A., Richter, W.J., and Vliegenthart, J.F. (1994) New type of linkage between a carbohydrate and a protein: C-glycosylation of a specific tryptophan residue in human RNase Us. *Biochemistry*, **33**, 13524–13530.

Hofsteenge, J., Huwiler, K.G., Macek, B., Hess, D., Lawler, J., Mosher, D.F., and Peter-Katalinic, J. (2001) C-mannosylation and O-fucosylation of the thrombospondin type 1 module. *J. Biol. Chem.*, **276**, 6485–6498.

Holmes, D.I.R., Wahab, N.A., and Mason, R.M. (1997) Identification of glucose-regulated genes in human mesangial cells by mRNA differentiation display. *Biochem. Biophy. Res. Commun.*, **238**, 179–184.

Horiuchi, K., Yonekawa, O., Iwahara, K., Kanno, T., Kurihara, T., and Fujise, Y. (1994) A hydrophilic tetrahydro-β-carboline in human urine. *J. Biochem. (Tokyo)*, **115**, 362–366.

Ihara, Y., Sakamoto, Y., Mihara, M., Shimizu, K., and Taniguchi, N. (1997) Overexpression of N-acetylglucosaminyltransferase III disrupts the tyrosine phosphorylation of Trk with resultant signaling dysfunction in PC12 cells treated with nerve growth factor. *J. Biol. Chem.*, **272**, 9629–9634.

Ihara, Y., Yasuoka, C., Kageyama, K., Wada, Y., and Kondo, T. (2002) Tyrosine phosphorylation of clathrin heavy chain under oxidative stress. *Biochem. Biophys. Res. Commun.*, **297**, 353–360.

Koya, D., Dennis, J.W., Warren, C.E., Takahara, N., Schoen, F.J., Nishio, Y., Nakajima, T., Lipes, M.A., and King, G.L. (1999) Overexpression of core 2 N-acetylglucosaminyltransferase enhances cytokine actions and induces hypertrophic myocardium in transgenic mice. *FASEB J.*, **13**, 2329–2337.

Kornfeld, R. and Kornfeld, S. (1985) Assembly of asparagine-linked oligosaccharides. *Annu. Rev. Biochem.*, **54**, 631–664.

Lawler, J. (2000) The functions of thrombospondin-1 and 2. *Curr. Opin. Cell Biol.*, **12**, 634–640.

Liu, K., Paterson, A.J., Chin, E., and Kudlow, E. (2000) Glucose stimulates protein modification by O-linked GlcNAc in pancreatic β cells: linkage of O-linked GlcNAc to β cell death. *Proc. Natl Acad. Sci. USA*, **97**, 2820–2825.

Lowe, J.B. and Marth, J.D. (2003) A genetic approach to mammalian glycan function. *Annu. Rev. Biochem.*, **72**, 643–691.

Manabe, S. and Ito, Y. (1999) Total synthesis of novel subclass of glycoamino acid structure motif: C2-α-C-mannosylpyranosyl-L-tryptophan. *J. Am. Chem. Soc.*, **121**, 9754–9755.

McClain, D.A., Lubas, W.A., Cooksey, R.C., Hazel, M., Parker, G.J., Love, D.C., and Hanover, J.A. (2002) Altered glycan-dependent signaling induces insulin resistance and hyperleptinemia. *Proc. Natl Acad. Sci. USA*, **99**, 10695–10699.

McGregor, B., Colon, S., Mutin, M., Chignier, E., Zech, P., and McGregor, J. (1994) Thrombospondin in human glomerulopathies. A marker of inflammation and early fibrosis. *Am. J. Pathol.*, **144**, 1281–1287.

Murphy, M., Godson, C., Cannon, S., Kato, S., Mackenzie, H.S., Martin, F., and Brady, H.R. (1999) Suppression subtractive hybridization identifies high glucose levels as a stimulus for expression of connective tissue growth factor and other genes in human mesangial cells. *J. Biol. Chem.*, **274**, 5830–5834.

Nakayama, T., Yoshizaki, A., Kawahara, N., Ohtsuru, A., Wen, C.Y., Fukuda, E., Nakashima, M., and Sekine I. (2004) Expression of Tie-1 and 2 receptors, and angiopoietin-1, 2 and 4 in gastric carcinoma; immunohistochemical analyses and correlation with clinicopathological factors. *Histopathology*, **44**, 232–239.

Nishikawa, T., Ishikawa, M., and Isobe, M. (1999) Synthesis of α-1-C-mannosyltryptophan derivative, naturally occurring C-glycosyl amino acid found in human ribonuclease. *Synlett.*, 123–125.

Nishikawa, T., Ishikawa, M., Wada, K., and Isobe, M. (2001) Total synthesis of a 1-C-mannosyltryptophan, a naturally occurring C-glycosyl amino acid. *Synlett.*, 945–947.

Nishio, Y., Warren, C.E., Buczek-Thomas, J.A., Rulfs, J., Koya, D., Aiello, L.P., Feener, E.P., Miller, T.B., Dennis, J.W., and King, G.L. (1995) Identification and characterization of a gene regulating enzymatic glycosylation which is induced by diabetes and hyperglycemia specifically in rat cardiac tissue. *J. Clin. Invest.*, **96**, 1759–1767.

Olson, B.A., Day, J.R., and Lapling, N.J. (1999) Age-related expression of renal thrombospondin 1 mRNA in F344 rats: resemblance to diabetes-induced expression in obese Zucker rats. *Pharmacology*, **58**, 200–208.

Parker, G., Taylor, R., Jones, D., and McClain, D. (2004) Hyperglycemia and inhibition of glycogen synthase in streptozotocin-treated mice. Role of O-linked N-acetylglucosamine. *J. Biol. Chem.*, **279**, 20636–20642.

Perez-Vilar, J., Randell, S.H., and Boucher, R.C. (2004) C-mannosylation of MUC5AC and MUC5B Cys subdomains. *Glycobiology*, **14**, 325–337.

Poczatek, M.H., Hugo, C., Darley-Usmar, V., and Murphy-Ullrich, J.E. (2000) Glucose stimulation of transforming growth factor-β bioactivity in mesangial cells is mediated by thrombospondin-1. *Am. J. Pathol.*, **157**, 1353–1363.

Schachter, H. and Brockhausen, I. (1989) The biosynthesis of branched O-glycans. *Symp. Soc. Exp. Biol.*, **43**, 1–26.

Semenkovich, C.F. and Heinecke, J.W. (1997) The mystery of diabetes and athrosclerosis. Time for a new prot. *Diabetes*, **46**, 327–334.

Sharma, C., Dalferes, E.R. Jr., Radhakrishnamurthy, B., DePaolo, C.J., and Berenson, G.S. (1987) Hepatic glycoprotein synthesis in streptozotocin diabetic rats. *Biochem. Int.*, **15**, 395–401.

Sigel, M.B., Sinha, Y.N., and VanderLaan, W.P. (1983) Production of antibodies by inoculation into lymph nodes. *Methods Enzymol.*, **93**, 3–12.

Spiro, R.G. (2002) Protein glycosylation: nature, distribution, enzymatic formation, and disease implications of glycopeptide bonds. *Glycobiology*, **12**, 43R–56R.

Spiro, R.G. and Spiro, M.J. (1971) Effect of diabetes on the biosynthesis of the renal glomerular basement membrane. Studies on the glucosyltransferase. *Diabetes*, **20**, 641–648.

Stenina, O.I., Krukovets, I., Wang, K., Zhou, Z., Forudi, F., Penn, M.S., Topol, E.J., and Plow, E.F. (2003) Increased expression of thrombospondin-1 in vessel wall of diabetic zucker rat. *Circulation*, **107**, 3209–3215.

Tada, H. and Isogai, S. (1998) The fibronectin production is increased by thrombospondin via activation of TGF-β in cultured human mesangial cells. *Nephron*, **79**, 38–43.

Takahira, R., Yonemura, K., Yonekawa, O., Iwahara, K., Kanno, T., Fujise, Y., and Hashida, A. (2001) Tryptophan glycoconjugate as a novel marker of renal function. *Am. J. Med.*, **110**, 192–197.

Tan, K., Duquette, M., Liu, J.-H., Dong, Y., Zhang, R., Joachimiak, A., Lawler, J., and Wang, J.-H. (2002) Crystal structure of the TSP-1 type 1 repeats: a novel layered fold and its biological implication. *J. Cell Biol.*, **159**, 373–382.

Tepperman, H.M., DeWitt, J., and Tepperman, J. (1983) The effects of streptozotocin diabetes on the activities of rat liver glycosyltransferases. *Diabetes*, **32**, 412–415.

Van Wagoner, R.M., Jompa, J., Tahir, A., and Ireland, C.M. (1999) Trypargine alkaloids from a previously undescribed eudistoma sp. ascidian. *J. Nat. Prod.*, **62**, 794–797.

Varki, A. (1993) Biological roles of oligosaccharides: all of the theories are correct. *Glycobiology*, **3**, 97–130.

Vosseller, K., Wells, L., Lane, M.D., and Hart, G.W. (2002) Elevated nucleocytoplasmic glycosylation by O-GlcNAc results in insulin resistance associated with defects in Akt activation in 3T3-L1 adipocytes. *Proc. Natl Acad. Sci. USA*, **99**, 5313–5318.

Wang, S., Wu, X., Lincoln, T.M., and Murphy-Ullrich, J.E. (2003) Expression of constitutively active cGMP-dependent protein kinase prevents glucose stimulation of thrombospondin 1 expression and TGF-b activity. *Diabetes*, **52**, 2144–2150.

Yevdokimova, N., Wahab, A.N., and Mason, R.M. (2001) Thrombospondin-1 is the key activator of TGF-β1 in human mesangial cells exposed to high glucose. *J. Am. Soc. Nephrol.*, **12**, 703–712.

Zachara, N.E. and Hart, G.W. (2004) O-GlcNAc a sensor of cellular state: the role of nucleocytoplasmic glycosylation in modulating cellular function in response to nutrition and stress. *Biochim. Biophys. Acta*, **1673**, 13–28.

Zucker, L.M. and Antoniades, H.N. (1972) Insulin and obesity in the Zucker genetically obese rat ifattyî. *Endocrinology*, **90**, 1320–1330.

Role of calreticulin in the sensitivity of myocardiac H9c2 cells to oxidative stress caused by hydrogen peroxide

Yoshito Ihara, Yoshishige Urata, Shinji Goto and Takahito Kondo

Am J Physiol Cell Physiol 290:208-221, 2006. First published Aug 31, 2005;
doi:10.1152/ajpcell.00075.2005

AJP - Cell Physiology is dedicated to innovative approaches to the study of cell and molecular physiology. It is published 12 times a year (monthly) by the American Physiological Society, 9650 Rockville Pike, Bethesda MD 20814-3991. ISSN: 0363-6143, ESSN: 1522-1563. Visit our website at http://www.the-aps.org/.

Am J Physiol Cell Physiol 290: C208–C221, 2006.
First published August 31, 2005; doi:10.1152/ajpcell.00075.2005.

Role of calreticulin in the sensitivity of myocardiac H9c2 cells to oxidative stress caused by hydrogen peroxide

Yoshito Ihara,[1,2] Yoshishige Urata,[1] Shinji Goto,[1] and Takahito Kondo[1]

[1]*Department of Biochemistry and Molecular Biology in Disease, Atomic Bomb Disease Institute, Nagasaki University Graduate School of Biomedical Sciences, Nagasaki; and* [2]*Core Research for Evolutional Science and Technology, Japan Science & Technology Agency, Kawaguchi, Japan*

Submitted 22 February 2005; accepted in final form 29 August 2005

Ihara, Yoshito, Yoshishige Urata, Shinji Goto, and Takahito Kondo. Role of calreticulin in the sensitivity of myocardiac H9c2 cells to oxidative stress caused by hydrogen peroxide. *Am J Physiol Cell Physiol* 290:. C208–C221, 2006. First published August 31, 2005; doi:10.1152/ajpcell.00075.2005.—Calreticulin (CRT), a Ca^{2+}-binding molecular chaperone in the endoplasmic reticulum, plays a vital role in cardiac physiology and pathology. Oxidative stress is a main cause of myocardiac apoptosis in the ischemic heart, but the function of CRT under oxidative stress is not fully understood. In the present study, the effect of overexpression of CRT on susceptibility to apoptosis under oxidative stress was examined using myocardiac H9c2 cells transfected with the *CRT* gene. Under oxidative stress due to H_2O_2, the CRT-overexpressing cells were highly susceptible to apoptosis compared with controls. In the overexpressing cells, the levels of cytoplasmic free Ca^{2+} ($[Ca^{2+}]_i$) were significantly increased by H_2O_2, whereas in controls, only a slight increase was observed. The H_2O_2-induced apoptosis was enhanced by the increase in $[Ca^{2+}]_i$ caused by thapsigargin in control cells but was suppressed by BAPTA-AM, a cell-permeable Ca^{2+} chelator in the CRT-overexpressing cells, indicating the importance of the level of $[Ca^{2+}]_i$ in the sensitivity to H_2O_2-induced apoptosis. Suppression of CRT by the introduction of the antisense cDNA of *CRT* enhanced cytoprotection against oxidative stress compared with controls. Furthermore, we found that the levels of activity of calpain and caspase-12 were elevated through the regulation of $[Ca^{2+}]_i$ in the CRT-overexpressing cells treated with H_2O_2 compared with controls. Thus we conclude that the level of CRT regulates the sensitivity to apoptosis under oxidative stress due to H_2O_2 through a change in Ca^{2+} homeostasis and the regulation of the Ca^{2+}-calpain-caspase-12 pathway in myocardiac cells.

apoptosis; calcium; endoplasmic reticulum

CALRETICULIN (CRT) is a Ca^{2+}-binding molecular chaperone expressed in the endoplasmic reticulum (ER) of a wide variety of eukaryotic cells (35). CRT is involved in many biological processes, including the regulation of Ca^{2+} homeostasis and intracellular signaling, glycoprotein folding, cell adhesion, gene expression, and nuclear transport (17, 23, 35).

CRT is well expressed in the embryonic rat heart, but its expression is suppressed after birth (21). It has been shown that CRT is essential for cardiac development in mice (33, 45). *CRT*-deficient embryonic cells showed an impaired nuclear import of nuclear factor of activated T-cell type 3 (NF-AT3), a transcription factor, indicating that CRT functions in cardiac development as a component of the Ca^{2+}/calcineurin/NF-AT/GATA-4 transcription pathway (33). On the other hand, *CRT*-transgenic mice experience complete heart block and sudden death (42). The CRT-dependent cardiac block involves an impairment of both the L-type Ca^{2+} channel and gap junction connexins 40 and 43 (Cx40 and Cx43, respectively). Also observed was a decrease in phosphorylated Cx43 in the *CRT*-transgenic heart, suggesting that the functions of protein kinases are altered via the regulation of Ca^{2+} homeostasis. CRT is also overexpressed in rat cardiomyocytes under pressure overload cardiac hypertrophy, implying some dysfunction of cardiomyocytes related to the overexpression (51). Furthermore, in cultured myocardiac H9c2 cells, overexpression of CRT after gene transfection promoted apoptosis during cardiac differentiation (24). In that study, the expression of protein phosphatase 2A (PP2A), a Ser/Thr protein phosphatase, was involved in altering the regulation of Akt signaling in H9c2 cells overexpressing CRT via an increase in the cytoplasmic free Ca^{2+} concentration ($[Ca^{2+}]_i$). Recently, we also reported that Akt signaling is important for cytoprotection against oxidative stress (39) and that a long-term change in $[Ca^{2+}]_i$ regulates *PP2Ac-α* gene transcription via the cAMP response element, resulting in a change in the activation status of Akt and leading to altered susceptibility to apoptosis (56). These studies suggest that CRT plays a vital role in myocardiac development and function, although the mechanism of this phenomenon has not been clarified fully.

An increasing body of evidence suggests that apoptosis plays an important role in cardiac development and disease (9, 12). Apoptosis occurs during reperfusion after ischemia in a variety of organs, including the heart (4). Oxidative stress with reactive oxygen species generated during ischemia-reperfusion injury is implied in the mechanism of cardiac damage (4). However, the biological significance of CRT expression levels in cardiomyocytes under oxidative stress has not been revealed to date.

In the present study, we have investigated the biological role of CRT using rat myocardiac H9c2 cells transfected with the *CRT* gene. We show that the level of CRT alters the sensitivity to apoptosis under oxidative stress with H_2O_2 through a change in Ca^{2+} homeostasis and Ca^{2+}-dependent signaling of the calpain-caspase-12 pathway in myocardiac cells.

MATERIALS AND METHODS

Materials. Antibodies against CRT, calnexin (CNX), binding protein (BiP; glucose-regulating protein 78, Grp78), and ER-specific protein 57 (ERp57)/Grp58 were purchased from Stressgen (Victoria,

Address for reprint requests and other correspondence: Y. Ihara, Dept. of Biochemistry and Molecular Biology in Disease, Atomic Bomb Disease Institute, Nagasaki Univ. Graduate School of Biomedical Sciences, 1-12-4 Sakamoto, Nagasaki 852-8523, Japan (e-mail: y-ihara@net.nagasaki-u.ac.jp).

The costs of publication of this article were defrayed in part by the payment of page charges. The article must therefore be hereby marked "*advertisement*" in accordance with 18 U.S.C. Section 1734 solely to indicate this fact.

BC, Canada). Antibodies against GAPDH, caspase-12, and caspase-3 were obtained from Chemicon International (Temecula, CA), Mo-BiTec (Gottingen, Germany), and Cell Signaling Technology (Beverly, MA), respectively. Peroxidase-conjugated secondary antibodies against IgG of rabbit and mouse were purchased from Dako (Glostrup, Denmark). The other reagents used in the study were all of high grade and were obtained from Sigma or Wako Pure Chemicals (Osaka, Japan).

Cell lines and culture. H9c2 cells, a clonal cell line derived from embryonic rat heart, were obtained from the American Type Culture Collection (no. CRL-1446). H9c2 cells that had been transfected with the expression vector for mouse *CRT* cDNA were described previously (24). Two cell lines (CRT-S2 and CRT-S8) expressing high levels of CRT protein were used in the study. A 0.6-kb restriction fragment with *Eco*RI containing the translation initiation site was cut from the vector pcDNA3.1/mCRT (24) and inserted in the reverse orientation into pcDNA3.1 (Invitrogen) to obtain antisense CRT (20). The antisense cDNA expression vector was also transfected into H9c2 cells to establish a cell line (CRT-AS) in which the expression of *CRT* was suppressed (20). The established cell lines were used between *passages 12* and *18*. Cells were cultured in DMEM supplemented with 10% FCS in a humidified atmosphere of 95% air-5% CO_2 at 37°C. To induce oxidative stress, cells were cultured with media containing different concentrations of H_2O_2.

Immunoblot analysis. Cultured cells were harvested and lysed in lysis *buffer A* (20 mM Tris·HCl, pH 7.2, 130 mM NaCl, and 1% Nonidet P-40) including protease inhibitors (in μM: 20 4-amidinophenylmethanesulfonyl fluoride, 50 pepstatin, and 50 leupeptin). Protein samples were electrophoresed on 10% SDS-polyacrylamide gels under reducing conditions and then transferred onto a nitrocellulose membrane as described previously (19). The membrane was blocked with 5% skim milk in Tris-buffered saline (TBS; in mM: 10 Tris·HCl, pH 7.5, and 150 NaCl) and then incubated at 4°C overnight with primary antibody in TBS containing 0.05% Tween 20. The blots were coupled with the peroxidase-conjugated secondary antibodies, washed, and then developed using the ECL detection kit (Amersham Biosciences) according to the manufacturer's instructions. The intensity of protein bands was quantified densitometrically, and the value was estimated relative to that for GAPDH.

Fluorescence microscopy. Cells (50,000/ml) were grown on Lab-Tek chamber slides (Nunc) for 24 h. They were fixed with 4% paraformaldehyde in PBS (pH 7.2) and permeabilized for 10 min with PBS containing 1% Triton X-100. The cells were then blocked with 1% BSA in PBS, incubated with the antibody for 1 h, and washed with PBS containing 1% BSA. The immunoreactive primary antibodies were visualized using FITC-conjugated anti-rabbit immunoglobulins (Cappel). After being washed, the stained cells were mounted in VectaShield medium. A Zeiss Axioskop2 (Zeiss, Jena, Germany) with illumination for epifluorescence was used for fluorescence microscopic analysis.

Cell viability assay. The viability of cultured cells was evaluated by performing a 3-(4,5-dimethylthiazol-2-yl)-2,5-diphenyltetrazolium bromide (MTT) assay as described previously (38). Cells (5,000–10,000) were placed into 100 μl of medium per well in 96-well plates and cultured overnight. After cells were treated with H_2O_2, 10 μl of 0.5% MTT solution was added and the cells were incubated for 4 h. The reaction was stopped by adding 100 μl of lysis *buffer B* (20% SDS and 50% *N,N*-dimethyl formamide, pH 4.7), and then cell viability was evaluated by measuring the absorbance at 570 nm using a microplate reader.

Lactate dehydrogenase release assay. After H_2O_2 treatment, the incubation medium was collected and centrifuged at 10,000 *g* for 20 min, and the supernatant was stored at 4°C for the lactate dehydrogenase (LDH) activity assay. In untreated cells, the medium was removed and the same volume of lysis *buffer A* was added to the cells. The cells were lysed by trituration and centrifuged as described above, and then the supernatant was used to assay the LDH activity of all cells. LDH activity was measured spectrophotometrically using an LDH assay kit (MTX "LDH"; Kyokuto Pharmaceutical, Tokyo, Japan) according to the manufacturer's instructions.

Apoptosis assay. Apoptosis was detected by performing flow cytometry using the terminal deoxynucleotidyltransferase-mediated dUTP nick-end labeling (TUNEL) method (11) with the ApopTag Plus fluorescein in situ apoptosis detection kit (Chemicon International) as described previously (56). Morphological changes of nuclei in apoptotic cells were also characterized using fluorescence microscopy. Cells (50,000/ml) were grown on Lab-Tek chamber slides for 24 h. After undergoing H_2O_2 treatment, cells were fixed with 4% paraformaldehyde in PBS. The cells were stained with 2 μg/ml Hoechst 33342 (Molecular Probes, Eugene, OR) in PBS for 5 min so that we could visualize the nuclei. After being rinsed with PBS, the slides were examined using fluorescence microscopy as described above.

Measurement of cytoplasmic free Ca^{2+}. $[Ca^{2+}]_i$ was measured using a dual-excitation wavelength spectrofluorophotometer (RF-5500; Shimadzu, Kyoto, Japan) with fura-2 essentially as described previously (6, 36), but with a slight modification. Briefly, cultured cells on glass coverslips were loaded with 5 μM fura-2 AM (Dojindo, Kumamoto, Japan) for 20 min in Earle's balanced salt solution (EBSS; in mM: 26 $NaHCO_3$, pH 7.4, 1 NaH_2PO_4, 5.4 KCl, 116 NaCl, 5.5 glucose, and 2 $CaCl_2$) in the presence of 0.01% Pluronic acid F-127. After being washed four times with EBSS, the coverglass was positioned at a 45° angle to both excitation and emission light paths in a quartz cuvette containing 3.5 ml of fresh EBSS. Fura-2 fluorescence was determined at 37°C using the spectrofluorophotometer operating at an emission wavelength of 505 nm and excitation wavelengths of 340 and 380 nm. The maximal signal (R_{max}) was obtained by adding ionomycin at a 4 μM final concentration. Subsequently, the minimal signal (R_{min}) was obtained by adding EGTA at a 10 mM final concentration, followed by Tris-free base to a 30 mM final concentration, to increase the pH to 8.3. R is the ratio (F_1/F_2) of the fluorescence of excitation at 340 nm and emission at 505 nm (F_1) to that of excitation at 380 nm and emission at 505 nm (F_2). The actual $[Ca^{2+}]$ was calculated as $K_d \times (R - R_{min})/(R_{max} - R) \times Sf2/Sb2$, with $K_d = 224$ nM (16). The Sf2-to-Sb2 ratio is the ratio of fura-2 fluorescence at 380 nm in Ca^{2+}-free medium to that in Ca^{2+}-replete medium.

Assays for uptake and release of Ca^{2+} in the cell. The uptake of Ca^{2+} was measured radiometrically using the Millipore filtration technique as described previously (49), with a slight modification. The cells were cultured with the medium containing H_2O_2 for the periods indicated and then washed with EBSS and cultured for 10 min in EBSS containing $^{45}Ca^{2+}$ (5 μCi/ml). Cells were detached from the culture wells using trypsinization buffer (0.25% trypsin and 0.02% EDTA in EBSS), and the cell suspension was filtered through a 0.45-μm nitrocellulose filter (Bio-Rad Laboratories, Hercules, CA) under vacuum conditions. The filters were rinsed twice with 0.5 ml of washing buffer (in mM: 10 HEPES, pH 7.4, 150 KCl, 2 EGTA, and 2.5 $MgCl_2$). $^{45}Ca^{2+}$ uptake was calculated by measuring radioactivity and standardized according to protein concentrations. For the $^{45}Ca^{2+}$ release assay, cells were cultured for 48 h with the medium containing $^{45}Ca^{2+}$ (1 μCi/ml). After being washed with EBSS, the cells were incubated with EBSS containing H_2O_2. Aliquots were collected at the time points indicated and centrifuged. The radioactivity was measured in the supernatant as the amount of Ca^{2+} released from the cell.

Enzyme assay. Caspase-12 activity was measured with Ala-Thr-Ala-Asp-7-amino-4-trifluoromethylcoumarin (AFC) as a substrate by using a caspase-12 fluorometric assay kit (BioVision, Mountain View, CA) according to the manufacturer's protocol. The assay is based on the detection of cleavage of the substrate, and the activity was quantified using a spectrofluorophotometer to measure fluorescence (excitation, 400 nm; emission, 505 nm) derived from free AFC. Calpain activity was measured using the calpain substrate succinyl-Leu-Leu-Val-Tyr-7-amino-4-methylcoumarin (Suc-Leu-Leu-Val-Tyr-AMC) as described by Glading et al. (13), with a slight modification.

Cultured cells were treated with or without H_2O_2 and/or thapsigargin and then harvested and washed with EBSS. Cells were resuspended in EBSS at 2.5×10^5 cells/ml and kept on ice for up to 1 h. In each sample, 250 μl were added to a 2.5-ml quartz cuvette with stirring and allowed to warm to 37°C in the spectrofluorophotometer. At time −1 min, ionomycin in DMSO was added to a final 2.5 μM concentration. DMSO alone was added as a control. At *time 0*, Suc-Leu-Leu-Val-Tyr-AMC was added to a final 50 μM concentration, and fluorescence (excitation, 360 nm; emission, 460 nm) was measured immediately for 3 min.

Statistical analysis. Statistical analysis was performed as previously recommended (6a) using Student's *t*-test or ANOVA (StatView software). Significance was set at $P < 0.05$.

RESULTS

Overexpression of CRT enhances cytotoxic sensitivity of H9c2 cells to oxidative stress caused by H_2O_2. Rat myocardiac H9c2 cells were transfected with the expression vector for mouse *CRT* cDNA to obtain cell lines overexpressing CRT (24). Figure 1*A* shows that the expression of CRT increased in the overexpressed cells to ~2.7-fold the level in the parental and mock-transfected (control) H9c2 cells. The transfection had no apparent effect on the expression of other ER proteins such as CNX, BiP, and ERp57. The intracellular localization of CRT was examined using indirect immunofluorescence. As shown in Fig. 1*B*, immunoreactive signals showed a perinuclear reticular pattern in all cases, including the control and CRT-overexpressing cells, although the signal intensity was increased in the transfectants compared with the control cells. To investigate the effect of overexpression of CRT on the cytotoxic sensitivity of H9c2 cells to oxidative stress, control and CRT-overexpressing cells were exposed to different concentrations of H_2O_2 for 1 h and then cell viability was examined by performing an MTT assay as described in MATERIALS AND METHODS. One hour of exposure to H_2O_2 caused cell damage in a dose-dependent manner, and the cytotoxic effect was enhanced more in the gene-transfected cells (i.e., CRT-S2 and CRT-S8) than in the controls (i.e., parental and control vector-transfected cells) (Fig. 2*A*, *left*). As shown in Fig. 2*A*, *right*, in CRT-overexpressing cells, the cell viability was markedly reduced after 1-h exposure to 50 μM H_2O_2, although less reduction was observed in control cells. However, in both control and gene-transfected cells, viability was similarly suppressed after 4 h of exposure to 50 μM H_2O_2. Next, control and CRT-overexpressing cells were exposed to different concentrations of H_2O_2 for 2 h, and then the cytotoxic effect of H_2O_2 was examined by assaying LDH release as described in MATERIALS AND METHODS. Two hours of exposure to H_2O_2 caused cell damage in a dose-dependent manner, and the cytotoxic effect was enhanced more in the gene-transfected cells than in the controls (Fig. 2*B*, *left*). In Fig. 2*B*, *right*, the cells were treated with 50 μM H_2O_2 for the periods indicated, and the LDH released into the medium was quantified and expressed as a ratio to the total intracellular LDH content. The LDH release was enhanced more in the gene-transfected cells than in the controls during the treatment. Figure 2*C* shows that morphological change was observed using phase-contrast microscopy in control and CRT-overexpressing cells treated with 50 μM H_2O_2 for 2 h. In gene-transfected cells treated with H_2O_2, the cell shape was apparently round and had shrunk along with some bleblike structure, although no change was observed in

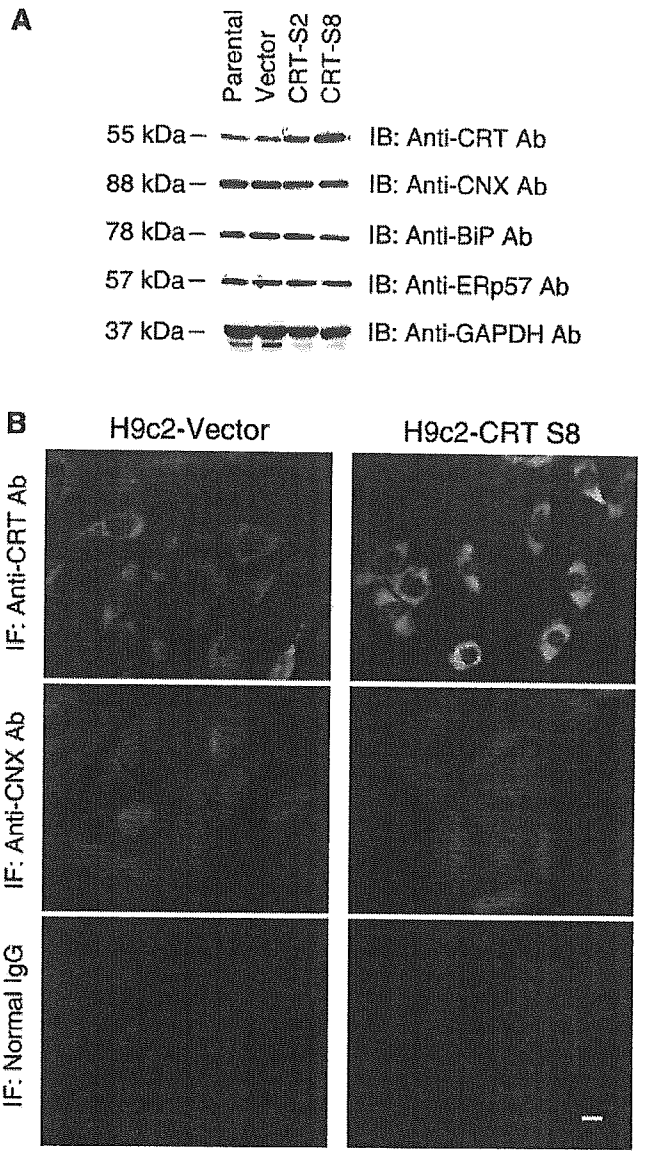

Fig. 1. *A*: expression levels for calreticulin (CRT), calnexin (CNX), binding protein (BiP; glucose-regulating protein 78, Grp78), ERp57/Grp58, and GAPDH were estimated in control (parental and vector) and *CRT* gene-transfected H9c2 (CRT-S2 and CRT-S8) cells using immunoblot analysis with specific antibodies (Ab) as described in MATERIALS AND METHODS. Data represent 3 independent experiments. *B*: intracellular localization of CRT and CNX was evaluated in control and *CRT* gene-transfected H9c2 cells using indirect immunofluorescence (IF) microscopy with specific antibodies. Background signals were obtained in cells stained with normal rabbit IgG. Data represent 3 independent experiments. Bar, 10 μm.

control cells treated with H_2O_2. Collectively, these results indicate that overexpression of CRT enhances the cytotoxic sensitivity to oxidative stress caused by H_2O_2 in myocardiac H9c2 cells.

Overexpression of CRT enhances apoptosis of H9c2 cells under oxidative stress due to H_2O_2. To examine whether apoptosis contributed to the cell damage observed in the transfectants under oxidative stress, a TUNEL assay was performed using cells treated with H_2O_2. In the study by Turner et

al. (52), maximal fragmentation of DNA was observed in H9c2 cells treated with 250 μM H_2O_2 for 4 h. We compared the extent of DNA strand breaks between control and gene-transfected cells treated with 50 μM H_2O_2 for 1 and 4 h. The TUNEL assay (Fig. 3*A*) showed that an increase in fluorescence intensity derived from DNA strand breaks in the transfectants but not in the control cells after H_2O_2 treatment. After the nucleus was stained with Hoechst 33342

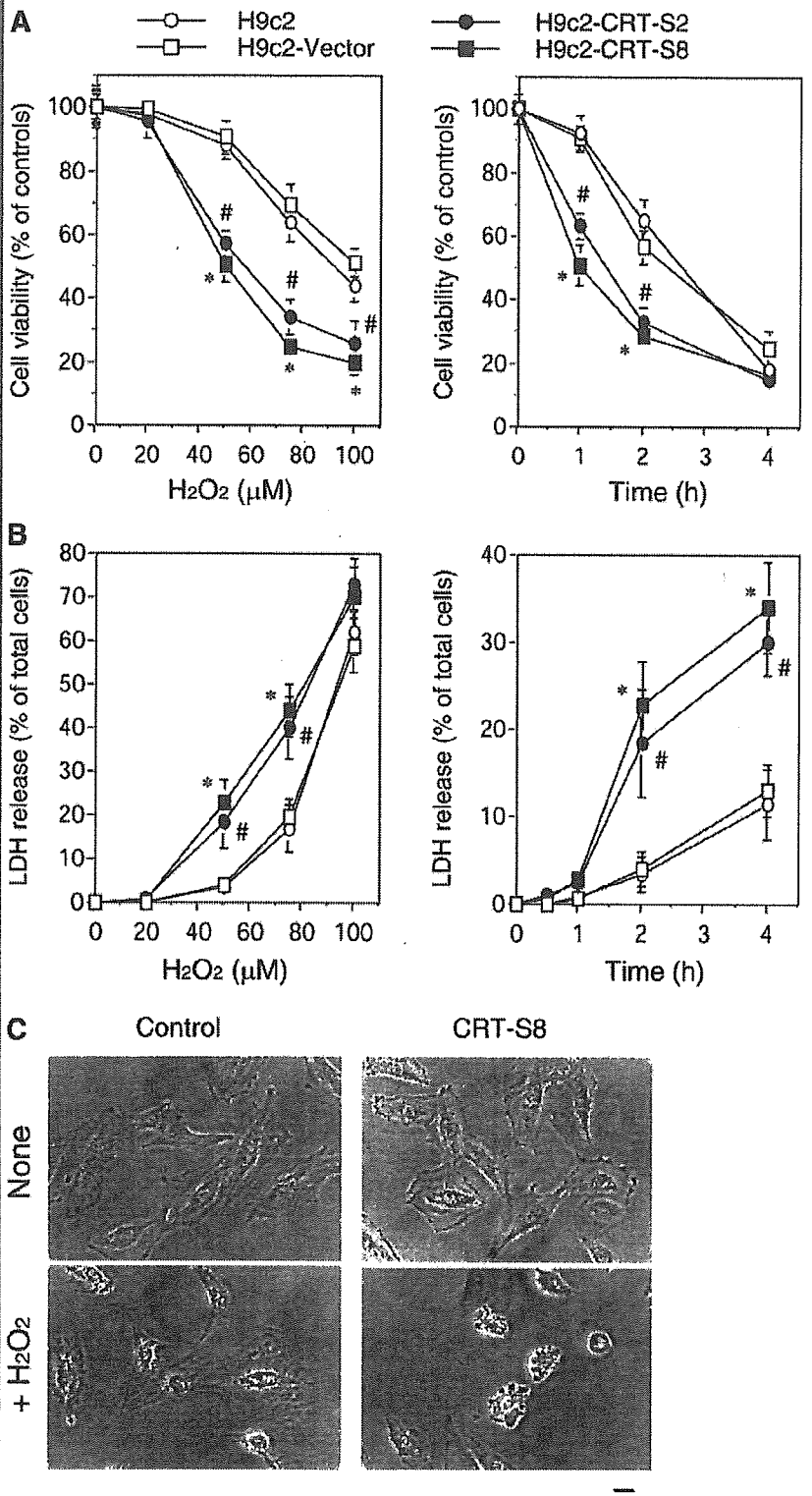

Fig. 2. Overexpression of CRT promotes cell damage in H9c2 cells under oxidative stress due to H_2O_2. *A*: control (H9c2 and H9c2-Vector) and *CRT* gene-transfected (H9c2-CRT-S2 and H9c2-CRT-S8) cells were exposed to different concentrations of H_2O_2 for 1 h, and then cell viability was examined by performing a 3-(4,5-dimethylthiazol-2-yl)-2,5-diphenyltetrazolium bromide (MTT) assay as described in MATERIALS AND METHODS (*left*). Cells were exposed to 50 μM H_2O_2 for the periods indicated, and then cell viability was examined by performing an MTT assay (*right*). Each value represents the mean ± SD of 4–6 independent experiments. Statistical analysis was performed using a factorial ANOVA test. $*P < 0.05$, $\#P < 0.05$ vs. value at same H_2O_2 concentration (*left*) or time point (*right*) for H9c2 cells treated with H_2O_2. *B*: control and *CRT* gene-transfected cells were exposed to different concentrations of H_2O_2 for 2 h, and then cell damage was examined by performing a lactate dehydrogenase (LDH) release assay as described in MATERIALS AND METHODS (*left*). Cells were treated with 50 μM H_2O_2 for the periods indicated, and the LDH released in the medium was quantified as described in MATERIALS AND METHODS and expressed as a percentage of total intracellular LDH content (*right*). Each value represents the mean ± SD of 4–6 independent experiments. $*P < 0.05$, $\#P < 0.05$ vs. value at same H_2O_2 concentration (*left*) or time point (*right*) as H9c2 cells treated with H_2O_2. *C*: control (H9c2-Vector), *CRT* gene-transfected (H9c2-CRT-S8) cells were exposed to 50 μM H_2O_2 for 2 h, and then cell morphology was examined using phase-contrast microscopy. Bar, 10 μm.

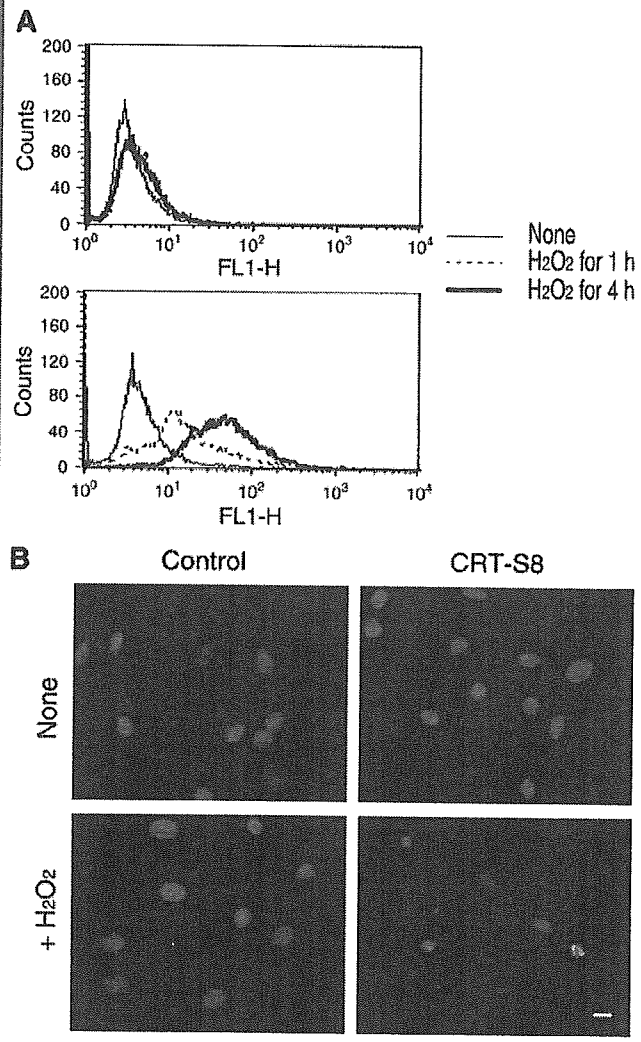

Fig. 3. Overexpression of CRT promotes apoptosis in H9c2 cells under oxidative stress due to H_2O_2. *A*: terminal deoxynucleotidyltransferase-mediated dUTP nick-end labeling (TUNEL) assay was performed for control (*top*) and gene-transfected (*bottom*) H9c2 cells under oxidative stress caused by H_2O_2. DNA strand breaks were detected using the TUNEL method as described in MATERIALS AND METHODS. Cells were treated with 50 μM H_2O_2 for the periods indicated. Data represent 3 independent experiments. *B*: morphological changes to nuclei were characterized in Hoechst-stained cells using a fluorescence microscope. Control and gene-transfected cells (50,000/ml) were grown on Lab-Tek chamber slides for 24 h and then treated with 50 μM H_2O_2 for 2 h. After being fixated with 4% paraformaldehyde in PBS, cells were stained with Hoechst 33342 and then visualized using fluorescence microscopy as described in MATERIALS AND METHODS. Bar, 10 μm.

(Fig. 3*B*), chromatin condensation and nuclear fragmentation were observed in the gene-transfected cells treated with H_2O_2, but not in the control cells treated with H_2O_2. Altogether, these results indicate that overexpression of CRT significantly enhances apoptosis in H9c2 cells under oxidative stress caused by H_2O_2.

Overexpression of CRT increases $[Ca^{2+}]_i$ in H9c2 cells under oxidative stress due to H_2O_2. To investigate whether the intracellular Ca^{2+} homeostasis was affected in the cells under oxidative stress, we measured $[Ca^{2+}]_i$ after H_2O_2 treatment (50 or 75 μM). To observe the effect of extracellular Ca^{2+} on $[Ca^{2+}]_i$, we treated the cells with H_2O_2 in the presence of 2 mM Ca^{2+} (+Ca^{2+}) or 10 mM EGTA (+EGTA). The measurement was based on the fluorescence intensity of cells loaded with fura-2 AM as described in MATERIALS AND METHODS. Figure 4 shows that in the presence of extracellular Ca^{2+} (+Ca^{2+}), control cells demonstrated no change in $[Ca^{2+}]_i$ level during treatment with 50 μM H_2O_2, but CRT-overexpressing cells increased to 180 nM after 35 min of treatment. Moreover, with 75 μM H_2O_2 treatment, the difference in the $[Ca^{2+}]_i$ increase was greater. On the other hand, in the absence of extracellular Ca^{2+} (+EGTA), the H_2O_2-induced $[Ca^{2+}]_i$ increase was not observed even in the CRT-overexpressing cells, suggesting that the increase was dependent on the influx of Ca^{2+} from the extracellular space. Altogether, the results indicate that $[Ca^{2+}]_i$ was apparently increased by oxidative stress due to H_2O_2 in CRT-overexpressing cells compared with controls, suggesting some modification of cellular Ca^{2+} homeostasis occurred because of CRT overexpression.

Alteration of Ca^{2+} flux in CRT-overexpressing H9c2 cells under oxidative stress. To investigate the effect of overexpression of CRT on Ca^{2+} influx in cells under oxidative stress, we examined the $^{45}Ca^{2+}$ uptake in control and *CRT* gene-trans-

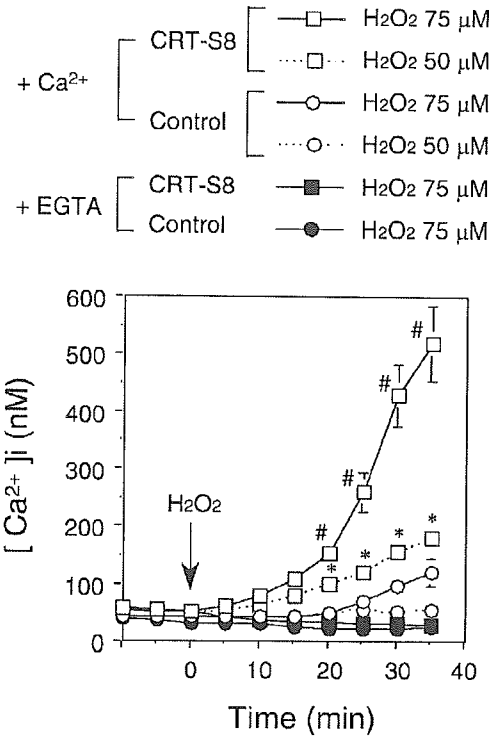

Fig. 4. Cytoplasmic free Ca^{2+} concentration ($[Ca^{2+}]_i$) increases in CRT-overexpressing H9c2 cells under oxidative stress due to H_2O_2. After being loaded with 5 μM fura-2 AM, control and gene-transfected cells cultured on glass coverslips were treated with H_2O_2 (50 or 75 μM) for the periods indicated. $[Ca^{2+}]_i$ was quantified by measuring fura-2 fluorescence as described in MATERIALS AND METHODS. To observe the effect of extracellular Ca^{2+} on $[Ca^{2+}]_i$, we treated the cells with H_2O_2 in the presence of 2 mM Ca^{2+} (+Ca^{2+}) or 10 mM EGTA (+EGTA). Each value represents the mean ± SD of 4 independent experiments. Statistical analysis was performed using a factorial ANOVA test. *$P < 0.05$ vs. value at same time point for control cells (Ca^{2+}) treated with 50 μM H_2O_2. #$P < 0.05$ vs. value at same time point for control cells (Ca^{2+}) treated with 75 μM H_2O_2.

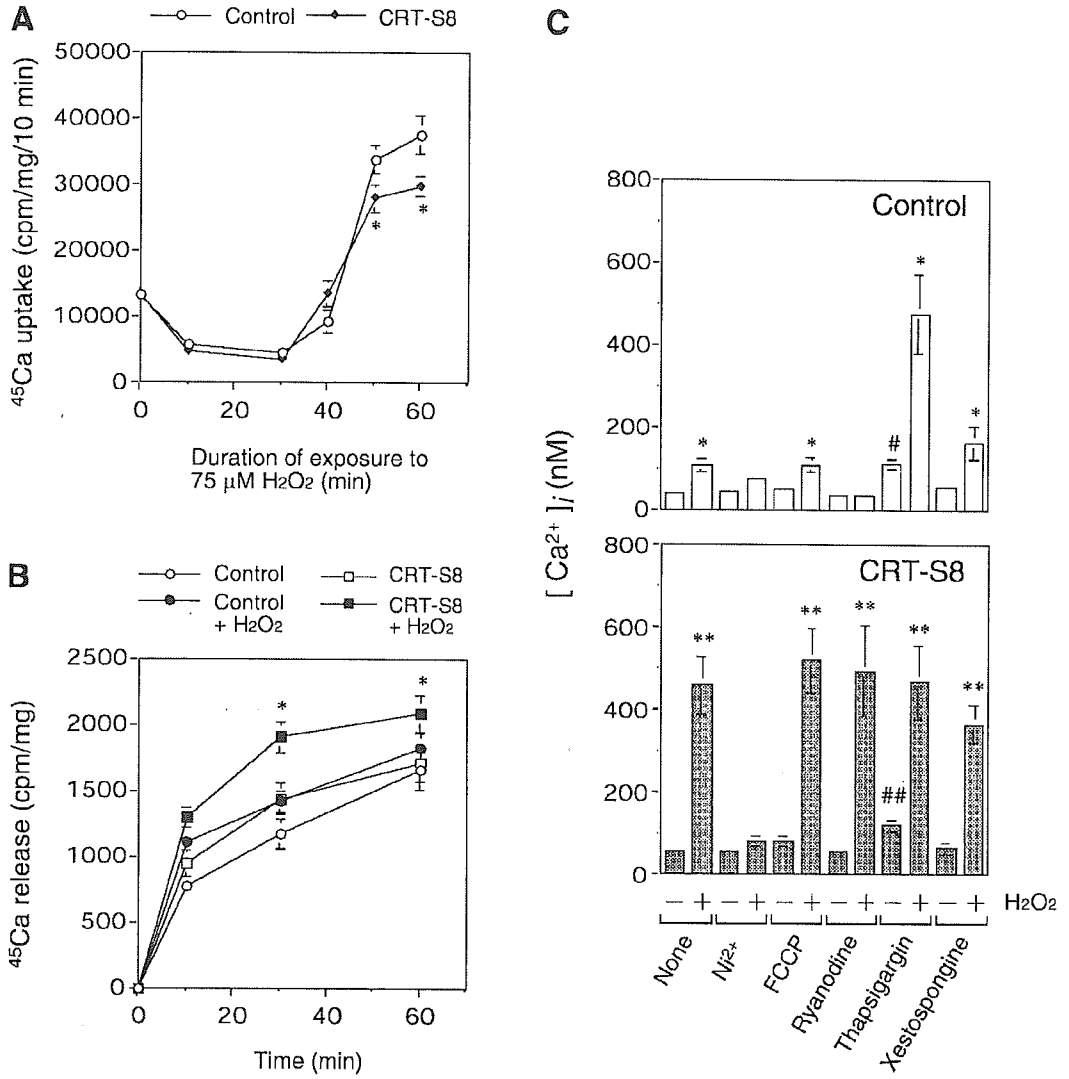

Fig. 5. *A*: uptake of Ca^{2+} in CRT-overexpressing H9c2 cells under oxidative stress due to H_2O_2. The cells were cultured with the medium containing 75 μM H_2O_2 for the indicated periods, washed with Earle's balanced salt solution (EBSS), and then cultured for 10 min in EBSS containing $^{45}Ca^{2+}$ (5 μCi/ml) as described in MATERIALS AND METHODS. After being washed with EBSS, the cells were harvested and $^{45}Ca^{2+}$ uptake was measured as described in MATERIALS AND METHODS. Each value represents mean ± SD of 3 independent experiments. Statistical analysis was performed using a factorial ANOVA test. $*P < 0.05$ compared with value at same time point for control cells treated with 75 μM H_2O_2. *B*: release of Ca^{2+} from CRT-overexpressing H9c2 cells under oxidative stress due to H_2O_2. Cells were cultured for 48 h with $^{45}Ca^{2+}$ as described in MATERIALS AND METHODS. After being washed with EBSS, the cells were incubated with EBSS containing 75 μM H_2O_2. Aliquots were collected at the time points indicated and then centrifuged. Radioactivity was measured in the supernatant as the amount of Ca^{2+} released from the cell. Each value represents mean ± SD of counts per minute (cpm) recovered in the supernatant normalized to the protein in the total cell pellets. $*P < 0.05$ vs. same time point for CRT-S8 cells treated without H_2O_2. *C*: effect of Ca^{2+} modulators on $[Ca^{2+}]_i$ in CRT-overexpressing H9c2 cells under oxidative stress with H_2O_2. After being loaded with 5 μM fura-2 AM, control and gene-transfected cells cultured on glass coverslips were pretreated with various modulators containing Ni^{2+} (5 mM), FCCP (1 μM), ryanodine (100 μM), thapsigargin (5 μM), and xestospongin C (1 μM) and then were treated with H_2O_2 (75 μM) for 30 min. $[Ca^{2+}]_i$ was quantified by measuring fura-2 fluorescence as described in MATERIALS AND METHODS. Each value represents mean ± SD of 3 independent experiments. $*P < 0.05$ vs. corresponding control cells treated without H_2O_2. $\#P < 0.05$ vs. untreated control cells (None). $**P < 0.05$ vs. corresponding CRT-S8 cells treated without H_2O_2. $\#\#P < 0.05$ vs. untreated CRT-S8 cells (None).

fected cells during treatment with 75 μM H_2O_2 as described in MATERIALS AND METHODS. As shown in Fig. 5*A*, in both control and gene-transfected cells, the rate of $^{45}Ca^{2+}$ uptake was suppressed within the first 30 min and then increased during oxidative stress. The uptake rate was higher in the control than in the gene-transfected cells after 40 min. Next, to investigate the effect of overexpression of CRT on Ca^{2+} efflux in the cell under oxidative stress, we examined the $^{45}Ca^{2+}$ release in control and gene-transfected cells during treatment with 75 μM H_2O_2 as described in MATERIALS AND METHODS. After being labeled with $^{45}Ca^{2+}$, the cells were treated with H_2O_2 and the amount of $^{45}Ca^{2+}$ released was measured as described in MATERIALS AND METHODS. As shown in Fig. 5*B*, although the amount of $^{45}Ca^{2+}$ released did not differ between untreated control and gene-transfected cells, the release was increased in gene-transfected cells compared with controls after 30-min treatment with H_2O_2. Collectively, in CRT-overexpressing cells, Ca^{2+} influx seemed to be suppressed and the efflux was

increased in the cells under oxidative stress caused by H_2O_2 compared with control cells treated with H_2O_2. Although these results were not consistent with the finding that $[Ca^{2+}]_i$ was highly elevated in gene-transfected cells treated with H_2O_2 (Fig. 4), they also suggested that an alteration of responses in the intracellular Ca^{2+} stores might lead to increased $[Ca^{2+}]_i$ in CRT-overexpressing cells.

Effect of Ca^{2+} modulators on $[Ca^{2+}]_i$ in CRT gene-transfected H9c2 cells under oxidative stress due to H_2O_2. To investigate whether intracellular Ca^{2+} pools contribute to the altered Ca^{2+} homeostasis, we examined the effect of Ca^{2+} modulators on $[Ca^{2+}]_i$ in cells treated with H_2O_2 (Fig. 5*C*). Ni^{2+} (5 mM) was used to block Ca^{2+} influx from the extracellular space via Ca^{2+} channels and Na^+/K^+ exchangers in the plasma membrane (26, 27). FCCP (1 μM) is a mitochondrial uncoupler that collapses the mitochondrial membrane potential that drives Ca^{2+} uptake into mitochondria (5). A high concentration of ryanodine (100 μM) was used as an antagonist for the ryanodine receptor (55). Thapsigargin (5 μM) was used to inhibit the function of sarco(endo)plasmic reticulum Ca^{2+}-ATPase (SERCA) to block the uptake of Ca^{2+} into the ER/sarcoplasmic reticulum (SR) (50). Xestospongin C (1 μM) is a cell-permeable inhibitor of the inositol 1,4,5-trisphosphate (IP_3) receptor (10). The cells were treated with each Ca^{2+} modulator for 10 min after being loaded with fura-2 AM and then were incubated with 75 μM H_2O_2 for 30 min, and $[Ca^{2+}]_i$ was measured as described in MATERIALS AND METHODS. The uptake of Ca^{2+} into mitochondria and the ER was disrupted by treatment with FCCP and thapsigargin, respectively. In control cells, FCCP did not enhance the H_2O_2-induced increase of $[Ca^{2+}]_i$. In CRT-overexpressing cells, $[Ca^{2+}]_i$ was similarly increased by H_2O_2 both cases, with and without FCCP. These results indicate no influence of FCCP on the H_2O_2-induced change of $[Ca^{2+}]_i$ in control and CRT-overexpressing cells. This finding also suggests that the enhancement of H_2O_2-induced increase of $[Ca^{2+}]_i$ observed in CRT-overexpressing cells may not be explained solely by dysfunction of mitochondrial Ca^{2+} uptake. In contrast, the H_2O_2-induced increase in $[Ca^{2+}]_i$ was apparently enhanced in control cells treated with thapsigargin. This indicates that the thapsigargin-sensitive pool (i.e., ER) is involved in the enhancement of H_2O_2-induced increase of $[Ca^{2+}]_i$ and also suggests that dysfunction of SERCA may have a promoting effect on the H_2O_2-induced increase of $[Ca^{2+}]_i$. The ryanodine and IP_3 receptors may be involved in the increase in $[Ca^{2+}]_i$ in response to H_2O_2. However, high concentrations of ryanodine and xestospongin C did not suppress the increase in $[Ca^{2+}]_i$ in CRT-overexpressing cells treated with H_2O_2, suggesting that the ryanodine and IP_3 receptors were not necessarily the main sources of the H_2O_2-induced increase of $[Ca^{2+}]_i$ in CRT-overexpressing cells. Furthermore, it was noteworthy that the H_2O_2-induced increase of $[Ca^{2+}]_i$ was clearly suppressed by Ni^{2+} in gene-transfected cells. This finding is also consistent with the result that the increase was inhibited in gene-transfected cells in the absence of extracellular Ca^{2+} (Fig. 4). These findings indicate that the influx of Ca^{2+} from the extracellular space is important for the H_2O_2-induced increase of $[Ca^{2+}]_i$ in CRT-overexpressing cells, despite the fact that the rate of influx was not increased in the gene-transfected cells treated with H_2O_2 (Fig. 5*A*). Altogether, these results indicate that the ER-stored Ca^{2+} pool plays an important role in the enhancement of the H_2O_2-induced increase of $[Ca^{2+}]_i$ in CRT-overexpressing cells, although Ca^{2+} influx from the extracellular space was also an important contributor to the increase.

$[Ca^{2+}]_i$ level is implicated in the susceptibility of H9c2 cells to apoptosis under oxidative stress due to H_2O_2. To determine whether the increase in $[Ca^{2+}]_i$ is part of the causative mechanism of apoptosis in the gene-transfected cells, H_2O_2-dependent cytotoxicity was examined in CRT-overexpressing cells in the presence or absence of BAPTA-AM, a cell-permeable Ca^{2+} chelator. As shown in Fig. 6*A*, *top*, cell viability was assessed by performing an MTT assay in gene-transfected cells exposed to H_2O_2 treatment (50 μM for 2 h) in the absence or presence of BAPTA-AM (10 μM). The viability was suppressed by H_2O_2 to 28.0 ± 3.4% of that in untreated cells in the absence of BAPTA-AM but returned to 50.5 ± 6.5% in its presence. As shown in Fig. 6*A*, *bottom*, cell damage was also assessed by performing a LDH release assay in gene-transfected cells exposed to H_2O_2 treatment (50 μM for 2 h) in the absence or presence of BAPTA-AM. The release was increased by H_2O_2 to 22.0 ± 5.4% that of untreated cells in the absence of BAPTA-AM but was remitted to 4.7 ± 2.5% in its presence. These results suggest that BAPTA-AM mitigates cell damage due to H_2O_2 by suppressing the increase of $[Ca^{2+}]_i$. The effect of BAPTA-AM on apoptosis was also examined using the TUNEL method in the gene-transfected cells after H_2O_2 treatment (Fig. 6*B*). In the absence of BAPTA-AM, TUNEL-positive cells increased after treatment with 50 μM H_2O_2 for 2 h but were not detected in the presence of BAPTA-AM even 2 h after treatment with H_2O_2. Conversely, the effect of an $[Ca^{2+}]_i$ increase on H_2O_2-induced apoptosis was examined in control H9c2 cells in the absence or presence of thapsigargin (5 μM), an inhibitor for SERCA (50). As shown in Fig. 6*C*, *top*, cell viability was suppressed by H_2O_2 (50 μM for 2 h) to 60.0 ± 4.4% of that in untreated cells in the absence of thapsigargin but was suppressed to 17.1 ± 4.6% in its presence. In Fig. 6*C*, *bottom*, cell damage was assessed by performing a LDH release assay in control cells exposed to H_2O_2 treatment (50 μM for 2 h) in the absence or presence of thapsigargin. The release was slightly increased by H_2O_2 to 7.5 ± 2.2% that of untreated cells in the absence of thapsigargin but was enhanced to 32.7 ± 2.5% in its presence. Furthermore, the effect of thapsigargin on apoptosis was examined using the TUNEL method in control cells with H_2O_2 treatment (Fig. 6*D*). In the presence of thapsigargin, TUNEL-positive cells increased in number after exposure to 50 μM H_2O_2 for 2 h, whereas in its absence, no increase was observed. These results suggest that thapsigargin enhances apoptosis caused by H_2O_2 treatment by increasing the $[Ca^{2+}]_i$ level. This finding was also consistent with our recently reported results (56). Altogether, these results indicate that the increase in $[Ca^{2+}]_i$ plays a causative role in the apoptosis of CRT-overexpressing cells under oxidative stress caused by H_2O_2.

Suppression of CRT expression by transfection with antisense CRT gene enhances cytoprotection of H9c2 cells against oxidative stress due to H_2O_2. To confirm whether the expression level of CRT influences susceptibility to oxidant-induced apoptosis in H9c2 cells, we transfected the cells with the antisense *CRT* gene expression vector and a cell line (CRT-AS) in which CRT expression was suppressed to a level lower than that in controls as described in MATERIALS AND METHODS (20). The expression level of CRT was compared with that in control

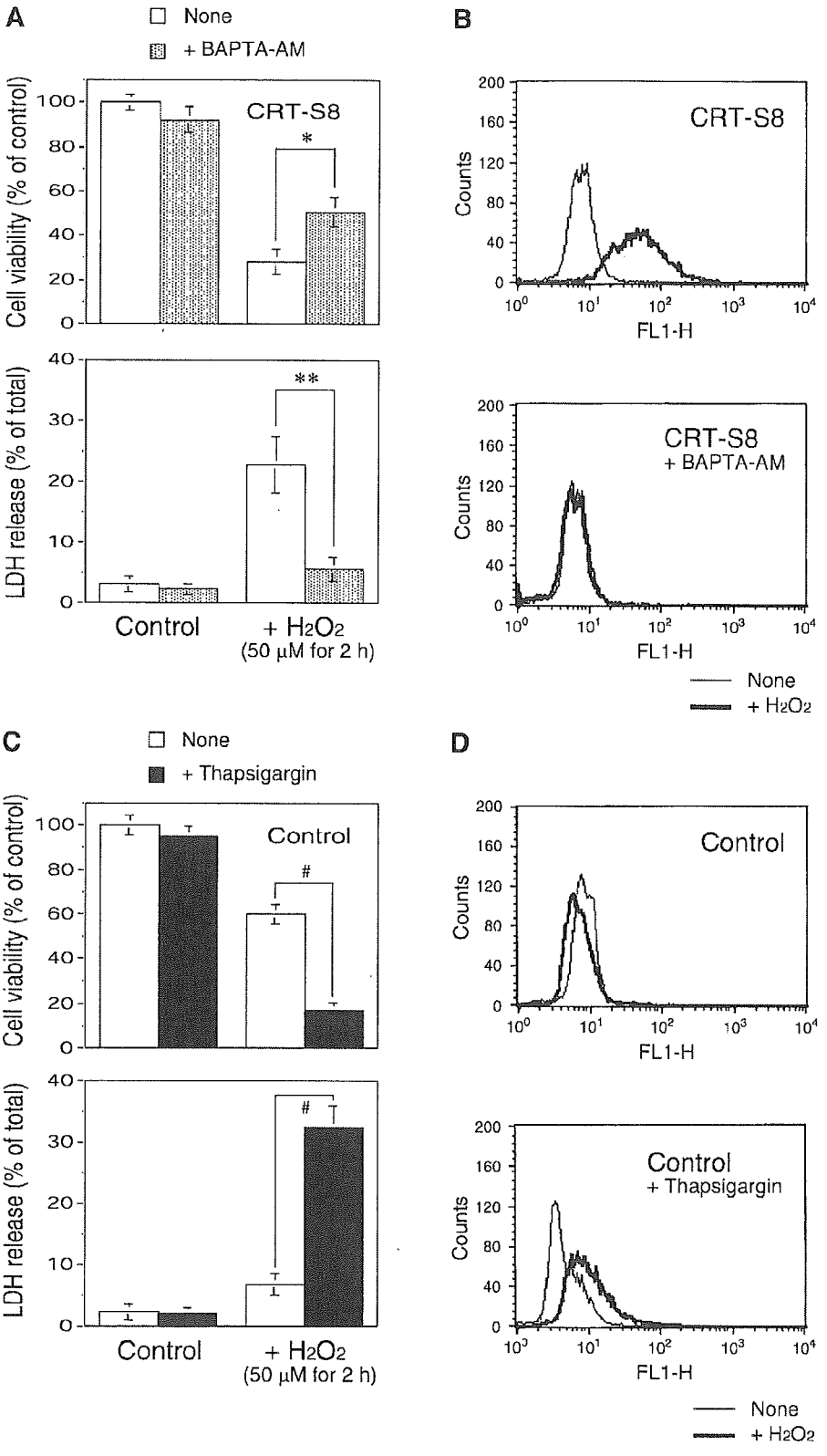

Fig. 6. Effect of Ca^{2+} modulators on apoptosis due to oxidative stress caused by H_2O_2. *A*: CRT-overexpressing (CRT-S8) cells were cultured in the presence or absence of 10 μM BAPTA-AM during the H_2O_2 treatment. The cells were exposed to 50 μM H_2O_2 for 2 h and then cell viability was examined by performing an MTT assay as described in MATERIALS AND METHODS. Each value represents the mean ± SD of 4 independent experiments. Statistical analysis was performed using a paired Student's *t*-test. $*P < 0.05$, $**P < 0.01$ vs. CRT-S8 cells treated with H_2O_2 without BAPTA-AM. *B*: TUNEL assay for CRT-overexpressing cells treated with or without BAPTA-AM and/or H_2O_2. Cells were cultured in the presence or absence of 10 μM BAPTA-AM during the H_2O_2 treatment. Thin line, no H_2O_2 for 2 h; thick line, 50 μM H_2O_2 for 2 h. DNA strand breaks were detected using the TUNEL method as described in MATERIALS AND METHODS. Data represent 3 independent experiments. *C*: control cells were cultured in the presence or absence of 5 μM thapsigargin during the H_2O_2 treatment. Cells were exposed to 50 μM H_2O_2 for 2 h, and then cell viability was examined by performing an MTT assay as described in MATERIALS AND METHODS. Each value represents the mean ± SD of 4 independent experiments. $\#P < 0.01$ vs. control cells treated with H_2O_2 without thapsigargin. *D*: TUNEL assay for control cells treated with or without thapsigargin and/or H_2O_2. Cells were cultured in the presence or absence of 5 μM thapsigargin during H_2O_2 treatment. Thin line, no H_2O_2 for 2 h; thick line, 50 μM H_2O_2 for 2 h. DNA double-stranded breaks were detected using the TUNEL method as described in MATERIALS AND METHODS. Data represent 4 independent experiments.

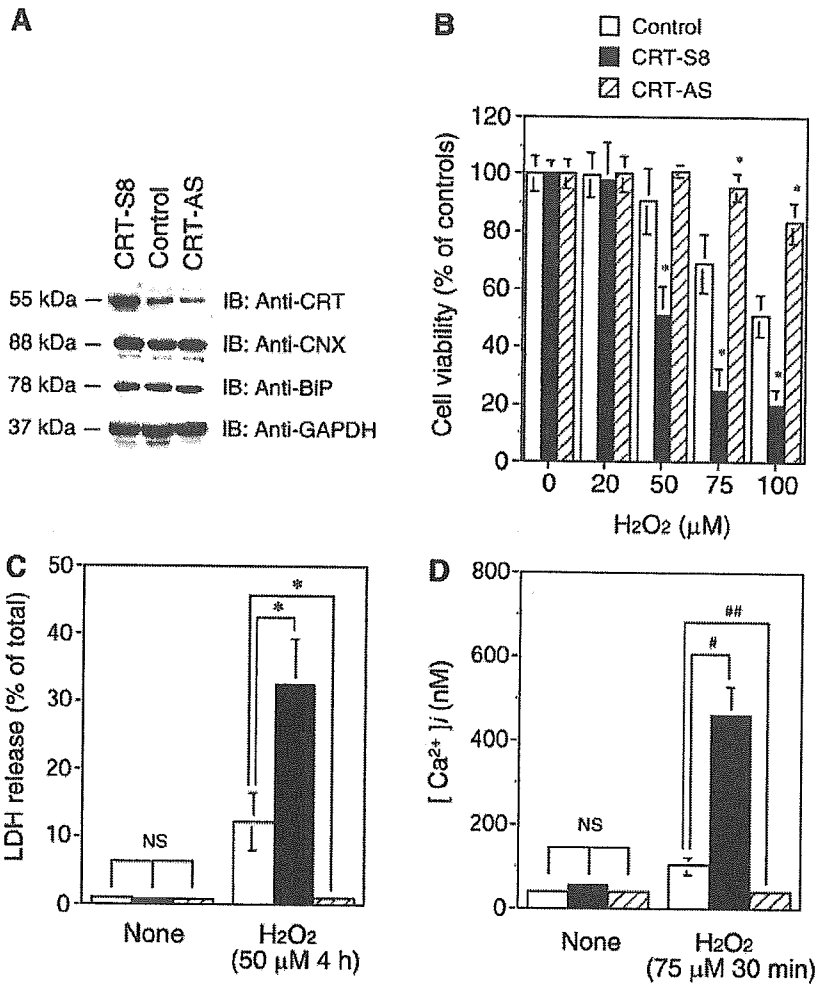

Fig. 7. Suppression of CRT expression showing cytoprotective effects in H9c2 cells under oxidative stress. To observe the effect of the suppressed expression of CRT on cytotoxicity under conditions of oxidative stress, we introduced the antisense gene for CRT into H9c2 cells to obtain cells underexpressing CRT as described in MATERIALS AND METHODS. *A*: expression levels of CRT, CNX, BiP, and GAPDH were examined in control, CRT-overexpressing (CRT-S8), and CRT-underexpressing (CRT-AS) cells using immunoblot analysis with specific antibodies. Data represent 4 independent experiments. *B*: control, CRT-overexpressing, and CRT-underexpressing cells were exposed to different concentrations of H_2O_2 for 1 h, and then cell viability was examined by performing an MTT assay as described in MATERIALS AND METHODS. Each value represents mean ± SD of 4 independent experiments. Statistical analysis was performed using a factorial ANOVA test. $*P < 0.05$ vs. same concentration of H_2O_2 for control cells treated with H_2O_2. *C*: control, CRT-overexpressing, and CRT-underexpressing cells were exposed to 50 μM H_2O_2 for 4 h, and then cell damage was examined by performing an LDH release assay as described in MATERIALS AND METHODS. Each value represents mean ± SD of 4 independent experiments. $*P < 0.01$ vs. control cells treated with H_2O_2. *D*: after being loaded with 5 μM fura-2 AM, control, CRT-overexpressing, and CRT-underexpressing cells cultured on glass coverslips were treated with 75 μM H_2O_2 for 30 min. $[Ca^{2+}]_i$ was quantified by measuring fura-2 fluorescence as described in MATERIALS AND METHODS. $\#P < 0.01$, $\#\#P < 0.05$ vs. control cells treated with H_2O_2.

and CRT-overexpressing cells by immunoblot analysis, and the results showed that the expression level was decreased to ~30% of the control level (Fig. 7*A*). Figure 7*B* shows that control, CRT-overexpressing, and CRT-underexpressing cells were exposed to different concentrations of H_2O_2 for 1 h, and then cell viability was examined by performing an MTT assay as described in MATERIALS AND METHODS. The results showed that cell viability was well maintained in CRT-underexpressing cells treated with H_2O_2 compared with the decreased viability in control and CRT-overexpressing cells. As shown in Fig. 7*C*, control, CRT-overexpressing, and CRT-underexpressing cells were exposed to 50 μM H_2O_2 for 4 h, and then the cytotoxic effect of H_2O_2 was also examined by assaying LDH release as described in MATERIALS AND METHODS. The results showed that the LDH release was suppressed more in CRT-underexpressing cells than in controls during the treatment, although the release was apparently increased in CRT-overexpressing cells. Altogether, the results show that suppression of CRT apparently enhanced cytoprotection against oxidative stress compared with controls, although overexpression of CRT increased the susceptibility to H_2O_2-induced cytotoxicity. This observation indicates that the expression level of CRT is a key factor in determining the susceptibility to H_2O_2-induced apoptosis in H9c2 cells. As shown in Fig. 7*D*, $[Ca^{2+}]_i$ was measured in control, CRT-overexpressing, and CRT-underexpressing cells after H_2O_2 treatment (75 μM) for 30 min. After the treatment with H_2O_2, the $[Ca^{2+}]_i$ increase was apparently suppressed in CRT-underexpressing cells compared with the increase in control and CRT-overexpressing cells. Collectively, the results indicate that the H_2O_2-induced $[Ca^{2+}]_i$ increase is influenced by the expression level of CRT in the cell.

Overexpression of CRT enhances processing and activation of caspase-12 through activation of calpain in H9c2 cells under oxidative stress due to H_2O_2. To further investigate the mechanism of the CRT-dependent enhancement of apoptosis through the alteration of Ca^{2+} homeostasis, we focused on caspase-12, which is activated by calpain, a Ca^{2+}-dependent cysteine protease, in ER stress-induced apoptosis (40). As shown in Fig. 8*A*, the expression levels of caspase-12 and caspase-3 and ER stress-related chaperones were examined using immunoblot analysis in control and CRT-overexpressing cells treated with 75 μM H_2O_2. In control cells, a pro-caspase form of caspase-12 (55 kDa) showed no change after 1 h of treatment with H_2O_2 but was diminished after 2 h of treatment. The level of 35-kDa proteolytic fragment of caspase-12 gradually increased during the 2-h treatment. In CRT-overexpressing cells, the level of the 55-kDa pro-caspase form was low and that of the 35-kDa fragment was rather high even under

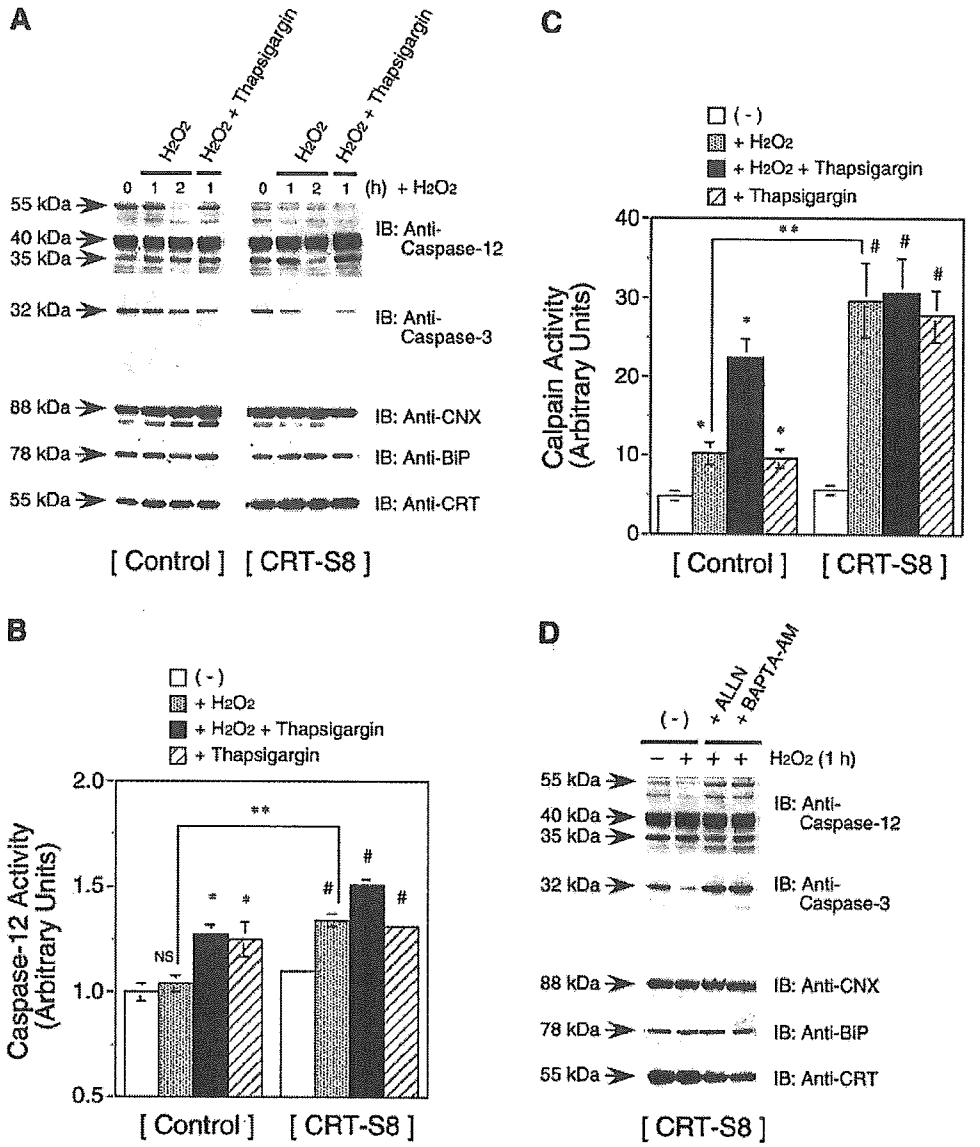

Fig. 8. The calpain-caspase-12 pathway is activated in CRT-overexpressing H9c2 cells under oxidative stress. *A*: control and CRT-overexpressing (CRT-S8) cells were exposed to 75 μM H_2O_2 for 1 and 2 h or to 75 μM H_2O_2 and 5 μM thapsigargin for 1 h, and then the expression levels of caspase-12 and caspase-3, CNX, BiP, and CRT were examined using cell lysates by performing immunoblot analysis with specific antibodies. Data represent 3 independent experiments. *B*: cells were exposed to 75 μM H_2O_2 and/or 5 μM thapsigargin for 1 h. Activity of caspase-12 was assayed with cell lysates using the substrate Ala-Thr-Ala-Asp-7-amino-4-trifluoromethylcoumarin (AFC) as described in MATERIALS AND METHODS. Each value represents the mean ± SD of 3 independent experiments. Statistical analysis was performed using a factorial ANOVA test. $*P < 0.05$ vs. untreated control cells. $**P < 0.05$ vs. control cells treated with H_2O_2. $\#P < 0.05$ vs. untreated CRT-S8 cells. NS, not significant vs. untreated control cells. *C*: cells were exposed to 75 μM H_2O_2 and/or 5 μM thapsigargin for 1 h. Activity of calpain was assayed using the calpain substrate succinyl-Leu-Leu-Val-Tyr-7-amino-4-methylcoumarin (Suc-Leu-Leu-Val-Tyr-AMC) as described in MATERIALS AND METHODS. Each value represents mean ± SD of 3 independent experiments. $*P < 0.05$ vs. untreated control cells. $**P < 0.05$ vs. control cells treated with H_2O_2. $\#P < 0.05$ vs. untreated CRT-S8 cells. *D*: CRT-overexpressing (CRT-S8) cells were treated for 1 h with or without 75 μM H_2O_2 in the presence or absence of 50 μM *N*-acetyl-leucyl-leucyl-norleucinal (ALLN) or 10 μM BAPTA-AM, and then the expression levels of caspase-12, caspase-3, CNX, BiP, and CRT were examined using cell lysates by performing immunoblot analysis with specific antibodies. Data represent 3 independent experiments.

nonstressed conditions. During treatment with H_2O_2, the 55-kDa band gradually decreased in intensity. On the other hand, the strength of the 35-kDa band was slightly increased after 1 h of treatment with H_2O_2 but was diminished after 2 h of treatment, suggesting enhanced proteolytic processing of the fragment in CRT-overexpressing cells treated with H_2O_2. The level of the 40-kDa band did not show significant change in control and CRT-overexpressing cells during treatment. These results indicate that proteolytic processing or degradation of caspase-12 was more accelerated in CRT-overexpressing cells than in control cells after treatment with H_2O_2. H_2O_2-induced processing also seemed to be enhanced by thapsigargin in both control and CRT-overexpressing cells. In the case of caspase-3, although the proteolytic cleavage was observed in control and CRT-overexpressing cells under stress due to H_2O_2, proteolysis was relatively accelerated in CRT-overexpressing cells

compared with controls. These results indicate that proteolytic processing or degradation of caspase-12 and caspase-3 is apparently accelerated in CRT-overexpressing cells under stress caused by H_2O_2. In contrast, no significant change in the expression levels of ER chaperones such as CNX, BiP, and CRT seemed to be induced by H_2O_2. Next, to investigate the relationship between proteolytic processing and the activity of caspase-12, we examined the enzyme activity of caspase-12 in cells after 1 h with or without 75 μM H_2O_2 and/or 5 μM thapsigargin (Fig. 8*B*). In CRT-overexpressing cells, activity was increased solely by H_2O_2, compared with no significant increase in activity in the control cells. Although activity was increased by thapsigargin in both control and CRT-overexpressing cells, it was elevated more in CRT-overexpressing cells during the combined treatment with H_2O_2. As shown in Fig. 8*C*, the activity of calpain was also examined in the cells after 1 h with or without 75 μM H_2O_2 and/or 5 μM thapsigargin. The activity of calpain was significantly increased by H_2O_2 in CRT-overexpressing cells compared with the small increase observed in control cells. In control cells, treatment with thapsigargin synergistically enhanced the effect of H_2O_2, although the activity was slightly increased solely by thapsigargin. In CRT-overexpressing cells, although calpain activity was markedly increased by thapsigargin, a synergistic effect was not observed. To determine whether the activity of calpain contributes to the processing of caspase-12, we examined the effect of *N*-acetyl-leucyl-leucyl-norleucinal (ALLN), a calpain inhibitor (57), or BAPTA-AM on processing in CRT-overexpressing cells during treatment with H_2O_2 (Fig. 8*D*). CRT-overexpressing cells were treated for 1 h with or without 75 μM H_2O_2 in the presence or absence of 50 μM ALLN or 10 μM BAPTA-AM, and then the expression levels of caspase-12 and caspase-3 and ER chaperones were examined using immunoblot analysis. The H_2O_2-induced processing of caspase-12 was apparently suppressed in the presence of ALLN or BAPTA-AM, resulting in a slight decrease in the level of the 35-kDa fragment and an increase in that of the 55-kDa procaspase form. Proteolytic processing of caspase-3 was also suppressed by ALLN or BAPTA-AM in gene-transfected cells treated with H_2O_2. Altogether, these results suggest that the Ca^{2+}-calpain pathway is involved in the activation of caspase-12 in CRT-overexpressing cells under oxidative stress caused by H_2O_2.

DISCUSSION

In the present study, we used myocardiac H9c2 cells that overexpressed CRT to investigate the effect of overexpression on H_2O_2-induced apoptosis in cardiac myocytes. When exposed to H_2O_2, the CRT-overexpressing cells showed increases in LDH release and DNA strand breaks, indicating that these cells were highly susceptible to apoptosis compared with control cells. Nakamura et al. (41) reported that overexpression of CRT resulted in increased sensitivity of HeLa cells to both thapsigargin- and staurosporine-induced apoptosis. These authors suggested that overexpression of CRT affected communication between the ER and the mitochondria to increase the sensitivity to apoptosis via the altered Ca^{2+} homeostasis, and their hypothesis has been supported by the study of Arnaudeau et al. (1). Pinton et al. (43) reported that the releasable $[Ca^{2+}]$ in the ER is important for ceramide-induced apoptosis and also showed that overexpression of CRT enhanced the ceramide-induced apoptosis in HeLa cells. Recently, it was also reported that CRT controls the susceptibility to apoptosis by regulating p53 functions (34). Furthermore, a necrosis-promoting effect of CRT has been reported to occur in *Caenorhabditis elegans* (53). In contrast, overexpression of CRT provided resistance to oxidant-induced cell death in renal epithelial LLC-PK1 cells treated with iodoacetamide (28), *tert*-butylhydroperoxide (29), or H_2O_2 (18). The function of CRT in the regulation of apoptosis may differ in specific cell types and is still controversial, so further investigation is required.

Ca^{2+} is one of the most versatile biological factors and regulates a variety of cellular events, such as cell development, cell proliferation, and cell death (3). The elevation of $[Ca^{2+}]_i$ has been thought to be an important signal in the mechanism of apoptosis (31). In the present study, we found that the level of $[Ca^{2+}]_i$ increased significantly in CRT-overexpressing cells treated with H_2O_2, although only a slight increase was observed in controls (Fig. 4). As shown in Fig. 6, H_2O_2-induced apoptosis was suppressed by the Ca^{2+} chelator BAPTA-AM in CRT gene-transfected cells but was promoted by thapsigargin in control cells, indicating that the increase in $[Ca^{2+}]_i$ was an important trigger for apoptosis in H9c2 cells under stress due to H_2O_2.

In previous reports, overexpression of CRT led to an increase in the intracellular store of Ca^{2+} (2, 8, 32, 54). CRT also appears to modulate store-operated Ca^{2+} influx (1, 2, 8, 32, 46, 54) and to alter Ca^{2+} transport by SERCA2b (22). In the case of H9c2 cells overexpressing CRT, the total cellular Ca^{2+} content examined on the basis of measuring equilibrium $^{45}Ca^{2+}$ uptake was ~160% of that in control cells and was found mainly within the thapsigargin-sensitive store. However, $[Ca^{2+}]_i$ levels in the resting state were not significantly different between control and CRT-overexpressing cells. On the other hand, store-operated Ca^{2+} influx was examined spectrofluorometrically using cells labeled with fura-2 AM and was suppressed in the CRT-overexpressing cells compared with controls (data not shown). These results indicate that overexpression of CRT influences intracellular Ca^{2+} homeostasis, and the effect in resting H9c2 cells seems to be similar to that in other cell types described in the literature. Recently, Scorrano et al. (48) reported that Ca^{2+} reserved in the ER was an important gateway for apoptosis via the influence on mitochondrial Ca^{2+} homeostasis. Overexpression of CRT also influences the mitochondrial Ca^{2+} homeostasis (1). Altogether, the enhanced susceptibility to H_2O_2-induced apoptosis in CRT-overexpressing H9c2 cells may also be due to the modulation of mitochondrial Ca^{2+} homeostasis by the altered responses in the ER overexpressing CRT.

Under oxidative stress, reactive oxygen and nitrogen can disrupt normal physiological pathways and cause cell death via altered Ca^{2+} homeostasis (7, 30). The $[Ca^{2+}]_i$ level is regulated by Ca^{2+} transport into and out of the ER or SR, in which Ca^{2+} can be stored, as well as by Ca^{2+} transport through the plasma membrane between the cytoplasm and the extracellular space (3). It was reported that oxidative stress causes a $[Ca^{2+}]_i$ increase in a variety of cell types (7). The initial increase in $[Ca^{2+}]_i$ results in part from a rapid release of ER Ca^{2+} through IP_3 receptors after receptor-mediated activation of PLC, and the subsequent generation of IP_3 and the sustained component results from the influx of extracellular Ca^{2+} (54). It is also

known that the uptake of Ca^{2+} from the cytoplasm to the ER/SR by SERCA can be inhibited by O_2^- and H_2O_2 in smooth muscle cells (14, 15). It seems that SERCA can be inhibited both by oxidation of its sulfhydryl residues and by a direct attack of oxidants on the ATP-binding site (7).

In the present study, the influx and efflux of $^{45}Ca^{2+}$ were examined in control and CRT-overexpressing cells with or without H_2O_2 treatment (Fig. 5, *A* and *B*). The results showed that Ca^{2+} influx was suppressed and that efflux was enhanced in the gene-transfected cells during H_2O_2 treatment, suggesting that the H_2O_2-induced increase in $[Ca^{2+}]_i$ might not be caused simply by the change of Ca^{2+} flux between the cytoplasm and extracellular space, but rather by the alteration in intracellular Ca^{2+} pools such as those in the ER and the mitochondria. To investigate the involvement of intracellular Ca^{2+} pools in the H_2O_2-induced increase in $[Ca^{2+}]_i$, we examined the effect of Ca^{2+} modulators on $[Ca^{2+}]_i$ in cells treated with H_2O_2 (Fig. 5*C*). The inhibition of mitochondrial function by FCCP did not enhance the H_2O_2-induced $[Ca^{2+}]_i$ increase in control cells, indicating that suppressed mitochondrial function was not a main cause of the enhancement of $[Ca^{2+}]_i$ observed in CRT-overexpressing cells. On the other hand, thapsigargin, an inhibitor for SERCA, apparently enhanced the H_2O_2-induced $[Ca^{2+}]_i$ increase in control cells, strongly suggesting that the Ca^{2+} store in the ER might be a cause of the $[Ca^{2+}]_i$ elevation observed in CRT-overexpressing cells. This observation also suggested that dysfunction of SERCA2a has a promoting effect on the H_2O_2-induced $[Ca^{2+}]_i$ increase in H9c2 cells. Although ER residents such as the ryanodine and IP_3 receptors may possibly be involved in raising $[Ca^{2+}]_i$ levels in response to H_2O_2, the inhibition of both did not suppress the H_2O_2-induced $[Ca^{2+}]_i$ increase in CRT-overexpressing cells. These results suggest that the H_2O_2-induced $[Ca^{2+}]_i$ increase may be due to a dysfunction of SERCA2a and not to the release of Ca^{2+} from the ER through the ryanodine or IP_3 receptors. However, it is noteworthy that the H_2O_2-induced increase of $[Ca^{2+}]_i$ was clearly suppressed by Ni^{2+}, an inhibitor of Ca^{2+} influx in gene-transfected cells. Collectively, these results indicate that the ER-stored Ca^{2+} pool plays an important role in the enhancement of the H_2O_2-induced $[Ca^{2+}]_i$ increase in CRT-overexpressing cells, although Ca^{2+} influx from the extracellular space was also an important contributor to the increase.

In a recently published report (15), we focused on the function of SERCA2a in CRT-overexpressing H9c2 cells under oxidative stress caused by H_2O_2 because SERCA is an ER/SR resident protein that is highly susceptible to peroxide stress. In that study, we found that in vitro activities of SERCA2a and $^{45}Ca^{2+}$ uptake into the ER were both suppressed by H_2O_2 in CRT-overexpressing H9c2 cells compared with controls (20). This finding indicates that the inactivation of SERCA2a was accelerated by the overexpression of CRT in the microsomes treated with H_2O_2. We also found that CRT transiently interacted with SERCA2a during H_2O_2-induced oxidative stress and that H_2O_2-induced degradation of SERCA2a was apparently enhanced in gene-transfected cells compared with controls. On the other hand, interaction between CRT and the IP_3 or ryanodine receptor was not detected in the cells under the same conditions (data not shown), suggesting that other Ca^{2+}-regulating proteins in the ER had little physical interaction with CRT under oxidative stress. These findings suggest that the increase in $[Ca^{2+}]_i$ may be due partly to the loss of Ca^{2+}-pumping activity of SERCA2a in the ER of CRT-overexpressing cells under oxidative stress.

Sustained elevation of the CRT level in the ER may be a consequence of ER stress. ER stress, also known as the unfolded protein response, is a physiological cellular response against accumulated misfolded proteins in the ER (25). However, prolonged ER stress is known to lead to apoptosis and to be linked to the pathogenesis of several disorders, including genetic diseases (e.g., type 1 diabetes mellitus), neurodegenerative diseases (e.g., Alzheimer disease, Parkinson disease), and metabolic diseases (e.g., hyperhomocysteinemia) (25). Caspase-12, which is associated with the ER, is specifically involved as a cell death effector via ER stress (40, 44). ER stress-induced activation of caspase-12 occurred through proteolytic processing by calpain via $[Ca^{2+}]_i$ elevation in the stressed cell (40). In the present study, we have shown that caspase-12 was highly activated in the CRT-overexpressing cells under oxidative stress through the activation of the Ca^{2+}-calpain pathway (Fig. 8). The results strongly suggest that a Ca^{2+}-calpain-caspase-12 pathway is involved in the mechanism of accelerated susceptibility to H_2O_2-induced apoptosis in CRT-overexpressing cells. Although Morishima et al. (37) did not clarify fully the precise activation mechanism for the caspase-12-related pathway, they reported that ER stress could trigger a specific cascade involving caspase-12, caspase-9, and caspase-3 in a cytochrome *c*-independent manner. This finding may be consistent with our findings that the H_2O_2-induced processing of both caspase-12 and caspase-3 was accelerated in CRT-overexpressing cells under stress and was suppressed in the presence of a calpain inhibitor, ALLN. Furthermore, the processing of caspase-12 and caspase-3 was suppressed by a Ca^{2+} chelator, BAPTA-AM, in the H_2O_2-treated, CRT-overexpressing cells, suggesting an activated linkage of the Ca^{2+}-calpain-caspase-12 signaling cascade in the apoptotic process of CRT-overexpressing cells under oxidative stress.

We also have shown that overexpression of CRT promotes apoptosis during cardiac differentiation in H9c2 cells (24). In that study, we showed that Akt signaling was suppressed in H9c2 cells overexpressing CRT via $[Ca^{2+}]_i$ increase. In addition, we recently reported (56) that cAMP response element-dependent transcriptional upregulation of the *PP2Ac-α* gene is involved in the inactivation of Akt, leading to the enhancement of oxidant-induced apoptosis in H9c2 cells under conditions in which $[Ca^{2+}]_i$ elevation is prolonged. With regard to the differentiation of cardiomyocytes, the importance of the intracellular generation of reactive oxygen species is implicated (47). In this respect, the altered Ca^{2+} homeostasis leading to accelerated apoptosis in CRT-overexpressing cells during differentiation may be related to a similar mechanism in cells to which reactive oxygen species are exposed. Moreover, in addition to the mechanism related to Akt signaling, the results of the present study also suggest that the Ca^{2+}-calpain-caspase-12 pathway is part of another mechanism of the differentiation-induced apoptosis of CRT-overexpressing H9c2 cells (24).

In conclusion, the results of the present study indicate that the level of CRT regulates susceptibility to oxidative stress through a change in Ca^{2+} homeostasis and a Ca^{2+}-dependent calpain-caspase-12 pathway in myocardiac H9c2 cells, suggesting a pathophysiological significance of CRT in myocardiac disorders under conditions of oxidative stress.

ACKNOWLEDGMENTS

We are grateful to Midori Ikezaki and Akiko Emura for technical assistance.

GRANTS

This work was supported in part by Grants-in-Aid for the 21st Century Centers of Excellence program from the Ministry of Education, Science, Sports, Culture, and Technology of Japan, and by grants from the Ministry of Health, Labor, and Welfare, Japan.

REFERENCES

1. **Arnaudeau S, Frieden M, Nakamura K, Castelbou C, Michalak M, and Demaurex N.** Calreticulin differentially modulates calcium uptake and release in the endoplasmic reticulum and mitochondria. *J Biol Chem* 277: 46696–46705, 2002.
2. **Bastianutto C, Clementi E, Codazzi F, Podini P, De Giorgi F, Rizzuto R, Meldolesi J, and Pozzan T.** Overexpression of calreticulin increases the Ca^{2+} capacity of rapidly exchanging Ca^{2+} stores and reveals aspects of their lumenal microenvironment and function. *J Cell Biol* 130: 847–855, 1995.
3. **Berridge MJ, Bootman MD, and Lipp P.** Calcium: a life and death signal. *Nature* 395: 645–648, 1998.
4. **Bishopric NH, Andreka P, Slepak T, and Webster KA.** Molecular mechanisms of apoptosis in the cardiac myocyte. *Curr Opin Pharmacol* 1: 141–150, 2001.
5. **Buckler KJ and Vaughan-Jones RD.** Effects of mitochondrial uncouplers on intracellular calcium, pH and membrane potential in rat carotid body type I cell. *J Physiol* 513: 819–833, 1998.
6. **Chen Q, Jones TW, and Stevens JL.** Early cellular events couple covalent binding of reactive metabolites to cell killing by nephrotoxic cysteine conjugates. *J Cell Physiol* 161: 293–302, 1994.

6a. **Curran-Everett D and Benos DJ.** Guidelines for reporting statistics in journals published by the American Physiological Society. *Am J Physiol Cell Physiol* 287: 243–245, 2004.

7. **Ermak G and Davies KJA.** Calcium and oxidative stress: from cell signaling to cell death. *Mol Immunol* 38: 713–721, 2001.
8. **Fasolato C, Pizzo P, and Pozzan T.** Delayed activation of the store-operated calcium current induced by calreticulin overexpression in RBL-1 cells. *Mol Biol Cell* 9: 1513–1522, 1998.
9. **Fisher SA, Langille BL, and Srivastava D.** Apoptosis during cardiovascular development. *Circ Res* 87: 856–864, 2000.
10. **Gafni J, Munsch JA, Lam TH, Catlin MC, Costa LG, Molinski TF, and Pessah IN.** Xestospongins: potent membrane permeable blockers of the inositol 1,4,5-trisphosphate receptor. *Neuron* 19: 723–733, 1997.
11. **Gavrieli Y, Sherman Y, and Ben-Sasson SA.** Identification of programmed cell death in situ via specific labeling of nuclear DNA fragmentation. *J Cell Biol* 119: 493–501, 1992.
12. **Gill C, Mestril R, and Samali A.** Losing heart: the role of apoptosis in heart disease—a novel therapeutic target? *FÁSEB J* 16: 135–146, 2002.
13. **Glading A, Chang P, Lauffenburger DA, and Wells A.** Epidermal growth factor receptor activation of calpain is required for fibroblast motility and occurs via an ERK/MAP kinase signaling pathway. *J Biol Chem* 275: 2390–2398, 2000.
14. **Grover AK and Samson SE.** Effect of superoxide radical on Ca^{2+} pumps of coronary artery. *Am J Physiol Cell Physiol* 255: C297–C303, 1988.
15. **Grover AK, Samson SE, and Fomin VP.** Peroxide inactivates calcium pumps in pig coronary artery. *Am J Physiol Heart Circ Physiol* 263: H537–H543, 1992.
16. **Grynkiewicz G, Poenie M, and Tsien RY.** A new generation of Ca^{2+} indicators with greatly improved fluorescence properties. *J Biol Chem* 260: 3440–3450, 1985.
17. **Holaska JM, Black BE, Love DC, Hanover JA, Leszyk J, and Paschal BM.** Calreticulin is a receptor for nuclear export. *J Cell Biol* 152: 127–140, 2001.
18. **Hung CC, Ichimura T, Stevens JL, and Bonventre JV.** Protection of renal epithelial cells against oxidative injury by endoplasmic reticulum stress preconditioning is mediated by ERK1/2 activation. *J Biol Chem* 278: 29317–29326, 2003.
19. **Ihara Y, Sakamoto Y, Mihara M, Shimizu K, and Taniguchi N.** Overexpression of *N*-acetylglucosaminyltransferase III disrupts the tyrosine phosphorylation of Trk with resultant signaling dysfunction in PC12 cells treated with nerve growth factor. *J Biol Chem* 272: 9629–9634, 1997.
20. **Ihara Y, Kageyama K, and Kondo T.** Overexpression of calreticulin sensitizes SERCA2a to oxidative stress. *Biochem Biophys Res Commun* 329: 1343–1349, 2005.
21. **Imanaka-Yoshida K, Amitani A, Ioshii SO, Koyabu S, Yamakado T, and Yoshida T.** Alteration of expression and distribution of the Ca^{2+}-sorting proteins in endo/sarcoplasmic reticulum during differentiation of rat cardiomyocytes. *J Mol Cell Cardiol* 28: 553–562, 1996.
22. **John LM, Lechleiter JD, and Camacho P.** Differential modulation of SERCA2 isoforms by calreticulin. *J Cell Biol* 142: 963–973, 1998.
23. **Johnson S, Michalak M, Opas M, and Eggleton P.** The ins and outs of calreticulin: from the ER lumen to the extracellular space. *Trends Cell Biol* 11: 122–129, 2001.
24. **Kageyama K, Ihara Y, Goto S, Urata Y, Toda G, Yano K, and Kondo T.** Overexpression of calreticulin modulates protein kinase B/Akt signaling to promote apoptosis during cardiac differentiation of cardiomyoblast H9c2 cells. *J Biol Chem* 277: 19255–19264, 2002.
25. **Kaufman RJ.** Orchestrating the unfolded protein response in health and disease. *J Clin Invest* 110: 1389–1398, 2002.
26. **Kimura J, Miyamae S, and Noma A.** Identification of sodium-calcium exchange current in single ventricular cells of guinea-pig. *J Physiol* 384: 199–222, 1987.
27. **Kurebayashi N and Ogawa Y.** Depletion of Ca^{2+} in the sarcoplasmic reticulum stimulates Ca^{2+} entry into mouse skeletal muscle fibres. *J Physiol* 533: 185–199, 2001.
28. **Liu H, Bowes RC III, van de Water B, Sillence C, Nagelkerke JF, and Stevens JL.** Endoplasmic reticulum chaperones GRP78 and calreticulin prevent oxidative stress, Ca^{2+} disturbances, and cell death in renal epithelial cells. *J Biol Chem* 272: 21751–21759, 1997.
29. **Liu H, Miller E, van de Water B, and Stevens JL.** Endoplasmic reticulum stress proteins block oxidant-induced Ca^{2+} increases and cell death. *J Biol Chem* 273: 12858–12862, 1998.
30. **Lounsbury KM, Hu Q, and Ziegelstein RC.** Calcium signaling and oxidant stress in the vasculature. *Free Radic Biol Med* 28: 1362–1369, 2000.
31. **McConkey DJ and Orrenius S.** The role of calcium in the regulation of apoptosis. *Biochem Biophys Res Commun* 239: 357–366, 1997.
32. **Mery L, Mesaeli N, Michalak M, Opas M, Lew DP, and Krause KH.** Overexpression of calreticulin increases intracellular Ca^{2+} storage and decreases store-operated Ca^{2+} influx. *J Biol Chem* 271: 9332–9339, 1996.
33. **Mesaeli N, Nakamura K, Zvaritch E, Dickie P, Dziak E, Krause KH, Opas M, MacLennan DH, and Michalak M.** Calreticulin is essential for cardiac development. *J Cell Biol* 144: 857–868, 1999.
34. **Mesaeli N and Phillipson C.** Impaired p53 expression, function, and nuclear localization in calreticulin-deficient cells. *Mol Biol Cell* 15: 1862–1870, 2004.
35. **Michalak M, Corbett EF, Mesaeli N, Nakamura K, and Opas M.** Calreticulin: one protein, one gene, many functions. *Biochem J* 344: 281–292, 1999.
36. **Morgan-Boyd R, Stewart JM, Vavrek RJ, and Hassid A.** Effects of bradykinin and angiotensin II on intracellular Ca^{2+} dynamics in endothelial cells. *Am J Physiol Cell Physiol* 253: C588–C598, 1987.
37. **Morishima N, Nakanishi K, Takenouchi H, Shibata T, and Yasuhiko Y.** An endoplasmic reticulum stress-specific caspase cascade in apoptosis: cytochrome *c*-independent activation of caspase-9 by caspase-12. *J Biol Chem* 277: 34287–34294, 2002.
38. **Mosmann T.** Rapid colorimetric assay for cellular growth and survival: application to proliferation and cytotoxicity assays. *J Immunol Methods* 65: 55–63, 1983.
39. **Murata H, Ihara Y, Nakamura H, Yodoi J, Sumikawa K, and Kondo T.** Glutaredoxin exerts antiapoptotic effect by regulating redox state of Akt. *J Biol Chem* 278: 50226–50233, 2003.
40. **Nakagawa T and Yuan J.** Cross-talk between two cysteine proteases: activation of caspase-12 by calpain in apoptosis. *J Cell Biol* 150: 887–894, 2000.
41. **Nakamura K, Bossy-Wetzel E, Burns K, Fadel MP, Lozyk M, Goping IS, Opas M, Bleackley RC, Green DR, and Michalak M.** Changes in endoplasmic reticulum luminal environment affect cell sensitivity to apoptosis. *J Cell Biol* 150: 731–740, 2000.
42. **Nakamura K, Robertson M, Liu G, Dickie P, Nakamura K, Guo JQ, Duff HJ, Opas M, Kavanagh K, and Michalak M.** Complete heart block and sudden death in mice overexpressing calreticulin. *J Clin Invest* 107: 1245–1253, 2001.
43. **Pinton P, Ferrari D, Rapizzi E, Di Virgilio F, Pozzan T, and Rizzuto R.** The Ca^{2+} concentration of the endoplasmic reticulum is a key deter-

minant of ceramide-induced apoptosis: significance for the molecular mechanism of Bcl-2 action. *EMBO J* 20: 2690–2701, 2001.

44. **Rao RV, Ellerby HM, and Bredesen DE.** Coupling endoplasmic reticulum stress to the cell death program. *Cell Death Differ* 11: 372–380, 2004.
45. **Rauch F, Prud'homme J, Arabian A, Dedhar S, and St-Arnaud R.** Heart, brain, and body wall defects in mice lacking calreticulin. *Exp Cell Res* 256: 105–111, 2000.
46. **Roderick HL, Llewellyn DH, Campbell AK, and Kendall JM.** Role of calreticulin in regulating intracellular Ca^{2+} storage and capacitative Ca^{2+} entry in HeLa cells. *Cell Calcium* 24: 253–262, 1998.
47. **Sauer H, Rahimi G, Hescheler J, and Wartenberg M.** Role of reactive oxygen species and phosphatidylinositol 3-kinase in cardiomyocyte differentiation of embryonic stem cells. *FEBS Lett* 476: 218–223, 2000.
48. **Scorrano L, Oakes SA, Opferman JT, Cheng EH, Sorcinelli MD, Pozzan T, and Korsmeyer SJ.** BAX and BAK regulation of endoplasmic reticulum Ca^{2+}: a control point for apoptosis. *Science* 300: 135–139, 2003.
49. **Sumida M and Tonomura Y.** Reaction mechanism of the Ca^{2+}-dependent ATPase of sarcoplasmic reticulum from the skeletal muscle: X. Direct evidence for Ca^{2+} translocation coupled with formation of a phosphorylated intermediate. *J Biochem (Tokyo)* 75: 283–297, 1974.
50. **Thastrup O, Cullen PJ, Drøbak BK, Hanley MR, and Dawson AP.** Thapsigargin, a tumor promoter, discharges intracellular Ca^{2+} stores by specific inhibition of the endoplasmic reticulum Ca^{2+}-ATPase. *Proc Natl Acad Sci USA* 87: 2466–2470, 1990.
51. **Tsutsui H, Ishibashi Y, Imanaka-Yoshida K, Yamamoto S, Yoshida T, Sugimachi M, Urabe Y, and Takeshita A.** Alteration in sarcoplasmic reticulum calcium-storing proteins in pressure-overload cardiac hypertrophy. *Am J Physiol Heart Circ Physiol* 272: H168–H175, 1997.
52. **Turner NA, Xia F, Azhar G, Zhang X, Liu L, and Wei JY.** Oxidative stress induces DNA fragmentation and caspase activation via the c-Jun NH_2-terminal kinase pathway in H9c2 cardiac muscle cells. *J Mol Cell Cardiol* 30: 1789–1801, 1998.
53. **Xu K, Tavernarakis N, and Driscoll M.** Necrotic cell death in *C. elegans* requires the function of calreticulin and regulators of Ca^{2+} release from the endoplasmic reticulum. *Neuron* 31: 957–971, 2001.
54. **Xu W, Longo FJ, Wintermantel MR, Jiang X, Clark RA, and DeLisle S.** Calreticulin modulates capacitative Ca^{2+} influx by controlling the extent of inositol 1,4,5-triphosphate-induced Ca^{2+} store depletion. *J Biol Chem* 275: 36676–36682, 2000.
55. **Yang F, He XP, Russell J, and Lu B.** Ca^{2+} influx-independent synaptic potentiation mediated by mitochondrial Na^{+}-Ca^{2+} exchanger and protein kinase C. *J Cell Biol* 163: 511–523, 2003.
56. **Yasuoka C, Ihara Y, Ikeda S, Miyahara Y, Kondo T, and Kohno S.** Antiapoptotic activity of Akt is down-regulated by Ca^{2+} in myocardiac H9c2 cells: evidence of Ca^{2+}-dependent regulation of protein phosphatase 2Ac. *J Biol Chem* 279: 51182–51192, 2004.
57. **Zhang L, Song L, and Parker EM.** Calpain inhibitor I increases β-amyloid peptide production by inhibiting the degradation of the substrate of γ-secretase: evidence that substrate availability limits β-amyloid peptide production. *J Biol Chem* 274: 8966–8972, 1999.

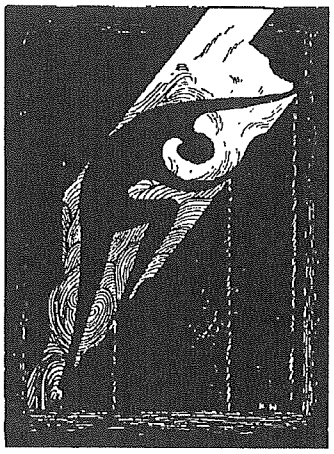

CHEST®

THE CARDIOPULMONARY
AND CRITICAL CARE JOURNAL

FOR PULMONOLOGISTS, CARDIOLOGISTS, CARDIOTHORACIC SURGEONS,
CRITICAL CARE PHYSICIANS, AND RELATED SPECIALISTS

Obstructive Sleep Apnea Causes Systemic Inflammation and Metabolic Syndrome

Shinji Teramoto, Hiroshi Yamamoto, Yasuhiro Yamaguchi, Ryoichi Namba and Yasuyoshi Ouchi

Chest 2005;127;1074-1075
DOI: 10.1378/chest.127.3.1074

appealing and correct, because CPET is both fun (to teach fellows about) and profitable (clinically), providing important diagnostic and clinical insight into pulmonary disease processes that cannot be obtained any other way. CPET is a test modality from which the attending physician will derive insight and benefit. As such, CPET is indeed profitable.

Charles G. Irvin, PhD
David A. Kaminsky, MD
University of Vermont
Burlington, VT

Correspondence to: Charles G. Irvin, PhD, The University of Vermont, Department of Medicine, College of Medicine, Division of Pulmonary Disease and Critical Care Medicine, 149 Beaumont Ave, Room 226, Burlington, VT 05405

REFERENCES

1 Irvin CG, Kaminsky DA. Exercise for fun and profit. Chest 2004; 125:1–3
2 Websters Seventh New Collegiate Dictionary. Springfield, MA: G. & C. Merriam Company, 1963
3 Irvin CG. To blow or not to blow: that is the question. Respir Care 2002; 47:1145–1146

Obstructive Sleep Apnea Causes Systemic Inflammation and Metabolic Syndrome

To the Editor:

In a recent issue of *CHEST* (July 2004),[1] Hatipoglu and Rubinstein pointed out that the possibilities of pathophysiologic link between obstructive sleep apnea syndrome (OSAS) and airway and/or systemic inflammation. They suggested that increased levels of tumor necrosis factor (TNF)-α, interleukin (IL)-6, and high-sensitivity C-reactive protein (hsCRP) are involved in the pathogenesis of systemic inflammation in OSAS. However, the important and growing issue of metabolic syndrome in patients with OSAS is not argued.

OSAS is recently recognized as a risk factor for cardiovascular disorders and metabolic syndrome.[2–6] OSAS is related to obesity, insulin resistance, and diabetes mellitus. In addition, leptin and insulin levels were elevated in patients with OSAS independently of obesity, and visceral fat was the primary parameter linked with sleep apnea. The association of OSAS with insulin resistance and diabetes type 2 has been confirmed.[5,6] Adiponectin is a hormone secreted by adipocytes that acts as an antidiabetic and antiatherogenic adipocytokine. Levels of adiponectin in the blood are decreased under conditions of obesity, insulin resistance, and type 2 diabetes. We have found that plasma level of adiponectin is decreased in OSAS patients compared with that in obese control subjects without OSAS.[7] The level of adiponectin is associated with the severity of OSAS as indicated by apnea-hypopnea index (AHI), rather than obesity indexed as body mass index. The lower adiponectin level is also associated with increased levels of hsCRP and IL-6.[7]

At the inflammatory point of view, the levels of TNF-α, IL-6, hsCRP, adhesion molecules, and monocyte chemoattractant protein-1 were markedly and significantly elevated in patients with sleep apnea than those in normal control subjects.[8,9] IL-6 and hsCRP levels were independently associated with OSAS severity as indicated by the AHI. In addition, hsCRP level is associated with visceral adipose tissue and is significantly associated with the components of insulin resistance syndrome.[5] These data support the belief that inflammatory processes and metabolic syndrome are activated in atherosclerotic lesions in patients with OSAS. C-reactive protein and other inflammatory cytokines accelerate the progression of atherosclerosis in patients with OSAS. In addition, increase in circulating levels of adenosine and urinary uric acid in patients with obstructive sleep apnea are implicated with increased production of reactive oxygen species. Activation of redox-sensitive gene expression is suggested by the increase in some protein products of these genes, including vascular endothelial growth factor, erythropoietin, endothelin-1, inflammatory cytokines, and adhesion molecules.[10,11] These results implicate the participation of redox-sensitive transcription factors as hypoxia-inducible factor-1, activator protein-1 and nuclear factor-κB.

Importantly, the elevated levels of atherogenic inflammatory mediators were improved by the OSAS-specific treatment such as nasal continuous positive airway pressure.[8–11] Thus, OSAS plays a crucial role in metabolic syndrome and systemic inflammatory disorders.

Shinji Teramoto, MD, FCCP
Hiroshi Yamamoto, MD
Yasuhiro Yamaguchi, MD
Ryoichi Namba, MD
Yasuyoshi Ouchi, MD
The University of Tokyo Hospital
Tokyo, Japan

This study was supported by the supported by a research grants from Japan Arteriosclerosis Prevention Fund and Danon Institute of Japan.
Correspondence to: Shinji Teramoto, MD, FCCP, Department of Geriatric Medicine, The University of Tokyo Hospital, 7–3–1 Hongo Bunkyo-ku, Tokyo 113-8655 Japan; e-mail: shinjit-tky@umin.ac.jp

REFERENCES

1 Hatipoglu U, Rubinstein I. Inflammation and obstructive sleep apnea syndrome: how many ways do I look at thee? Chest 2004; 126:1–2
2 Teramoto S, Ohga E, Ouchi Y. Obstructive sleep apnoea. Lancet 1999; 354:1213–1214
3 Teramoto S, Kume H, Matsuse T, et al. The risk of future cardiovascular diseases in the patients with OSAS is dependently or independently associated with obstructive sleep apnoea. Eur Respir J 2001; 17:573–574
4 Teramoto S, Kume H, Matsuse T. Ambulatory blood pressure after sleep apnoea treatment. Lancet 2002; 360:341–342
5 Coughlin SR, Mawdsley L, Mugarza JA, et al. Obstructive sleep apnoea is independently associated with an increased prevalence of metabolic syndrome. Eur Heart J 2004; 25:735–741
6 Harsch IA, Schahin SP, Radespiel-Troger M, et al. Continuous positive airway pressure treatment rapidly improves insulin sensitivity in patients with obstructive sleep apnea syndrome. Am J Respir Crit Care Med 2004; 169:156–162
7 Teramoto S, Yamamoto H, Yamaguchi Y, et al. A significant association of plasma adiponectin level with apnea-hypopnea index rather than BMI in patients with obstructive sleep apnea syndrome [abstract]. Am J Respir Crit Care Med 2004; 169:A430
8 Teramoto S, Yamamoto H, Ouchi Y. Increased C-reactive protein and increased plasma interleukin-6 may synergistically affect the progression of coronary atherosclerosis in obstructive sleep apnea syndrome [letter]. Circulation 2003; 107:E40

9 Alexandros N, Vgontzas, Dimitris A, et al. Sleep apnea and daytime sleepiness and fatigue: relation to visceral obesity, insulin resistance, and hypercytokinemia. J Clin Endocrinol Metab 2000; 85:1151–1158
10 Teramoto S, Kume H, Yamamoto H, et al. Effects of oxygen administration on the circulating vascular endothelial growth factor (VEGF) levels in patients with obstructive sleep apnea syndrome. Intern Med 2003; 42:681–685
11 Ohga E, Tomita T, Wada H, et al. Effects of obstructive sleep apnea on circulating ICAM-1, IL-8, and MCP-1. J Appl Physiol 2003; 94:179–184

Insights of Neurologic Dysfunction After Coronary Artery Bypass Grafting

To the Editor:

We read with great interest the article by Ganushchak and associates (June 2004).[1] The authors have investigated the correlation between the combinations of hemodynamic events during cardiopulmonary bypass (CPB) and the development of postoperative neurologic complications. The authors have utilized cluster analysis to review 1,395 perfusion charts, and have concluded that CPB procedures with large fluctuations in hemodynamic parameters have an increased risk for the development of postoperative neurologic complications.

We would like to make a few comments for this important investigation. First, it is well documented that the number of emboli (micro and macro) delivered during CPB has a direct correlation with the postoperative neurologic dysfunction.[2,3] The duration of CPB also has an impact on the number of emboli delivered during CPB; the longer the duration, more emboli delivered.[4] According to Table 2, the duration of CPB was much longer in one group with postoperative neurologic complications (n = 27) compared to the no-complication group (103 ± 43 min vs 82 ± 33 min, p = 0.01 [± SD]). The only way to quantify the number of microemboli during CPB is to use transcranial Doppler (TCD) monitoring. Did Ganushchak and associates use TCD monitoring during CPB?

Second, the authors have used two different hollow-fiber membrane oxygenators in this investigation. One wonders whether or not there was any significant difference between the oxygenators in 27 patients with postoperative neurologic complications. In 27 patients, did the authors calculate how many times one oxygenator was used vs the other oxygenator? Were there any significant differences between the two oxygenators?

Last, the authors have documented that the majority of patients with postoperative neurologic complications (21 of 27 patients) coincide with postoperative cardiac arrhythmias. It is not clear whether the neurologic complications were secondary to cardiac arrhythmias or not. The cause of postoperative neurologic complications in these 21 patients was probably due to ventricular arrhythmias rather the CPB procedure.[5] We congratulate the authors for applying cluster analysis to this particular patient population, and we also believe that large fluctuations in hemodynamic parameters during CPB has caused significant postoperative neurologic risks.[5]

Jun Luo, MD, PhD
Akif Ündar, PhD
Penn State College of Medicine
Hershey, PA

Correspondence to: Akif Ündar, PhD, Associate Professor of Pediatrics, Surgery, and Bioengineering, Penn State College of Medicine, Department of Pediatrics–H085, 500 University Dr. PO Box 850; Hershey, PA 17033-0850; e-mail: aundar@psu.edu

References

1 Ganushchak YM, Fransen EJ, Visser C, et al. Neurological complications after coronary artery bypass grafting related to the performance of cardiopulmonary bypass. Chest 2004; 125:2196–2205
2 Blaut CI. Macroemboli and microemboli during cardiopulmonary bypass. Ann Thorac Surg 1995; 59:1300–1303
3 Barbut D, Lo YW, Gold JP, et al. Impact of embolization during coronary artery bypass grafting on outcome and length of stay. Ann Thorac Surg 1997; 63:998–1002
4 Brown WR, Moody DM, Challa VR, et al. Longer duration of cardiopulmonary bypass is associated with greater numbers of cerebral microemboli. Stroke 2000; 31:707–713
5 Luo J, Zhu X, Xiao M, et al. Clinical analyses of determinants of perioperative mortality and complications after cardiac valve replacement. Chin Circ J 1996; 11:159–163

To the Editor:

First, we thank Drs. Luo and Ündar for their comments on our investigation, and acknowledge them for recognizing the interest and importance of our article. In answer to the first comment, we like to express that we also recognize the fact that the number of emboli (micro and macro) delivered during cardiopulmonary bypass (CPB) could have an impact on the incidence of postoperative neurologic complications. Unfortunately, we were unable to use transcranial Doppler (TCD) routinely in our patients. However, a longer CPB procedure is theoretically accompanied by a higher number of emboli delivered, as was described previously.[1,2] Therefore, although we did not use TCD, one could hypothesize that the aforementioned is confirmed by our findings as presented in Table 2. However, the large difference in number of patients in our study (27 patients with postoperative neurologic complications vs 1,368 patients without neurologic complications) made the results of the analysis of variance test suspicious. That is why we used cluster analyses, and in the sequence of these analyses the impact of duration of CPB on the development of postoperative neurologic complications disappeared. Nevertheless, microremobilization of cerebral vessels during CPB could be one of the factors explaining the significance of fluctuations in hemodynamic parameters in the increased risk for the development of postoperative neurologic complications. It is well documented that good blood flow through the brain might hasten the clearance of microemboli, and increased perfusion pressure during CPB has been proposed as a means of forcing air bubbles through the cerebral microcirculation.[3] It is obvious that fluctuations in perfusion pressure could often provoke the stabilization of an embolus in a cerebral vessel and increase the duration of hypoxia and extend the area of hypoxic damage.

Second, the type of oxygenator indeed could affect the rate of microemboli during CPB[4] and, in this way, be related to the incidence of postoperative neurologic complications. The two types of oxygenators used in our patients were used in sequence. Although the influence of oxygenator type on postoperative neurologic complications was beyond the scope of our study, we evaluated whether there was any significant fluctuation in the frequency of neurologic complications during the study period (between May 1996 and January 1999). This appeared not to be the case, and therefore we assumed that the type of oxygenator had no significant impact on the results as described in our article.

Third, in general, causal relations are extremely hard to prove in clinical research. In this retrospective study, we could not distinguish the sequence of events in complications development.